



CMS-SUS-13-024

CERN-PH-EP/2014-073
2014/08/19

Search for top-squark pairs decaying into Higgs or Z bosons in pp collisions at $\sqrt{s} = 8 \text{ TeV}$

The CMS Collaboration^{*}

Abstract

A search for supersymmetry through the direct pair production of top squarks, with Higgs (H) or Z bosons in the decay chain, is performed using a data sample of proton-proton collisions at $\sqrt{s} = 8 \text{ TeV}$ collected in 2012 with the CMS detector at the LHC. The sample corresponds to an integrated luminosity of 19.5 fb^{-1} . The search is performed using a selection of events containing leptons and bottom-quark jets. No evidence for a significant excess of events over the standard model background prediction is observed. The results are interpreted in the context of simplified supersymmetric models with pair production of a heavier top-squark mass eigenstate \tilde{t}_2 decaying to a lighter top-squark mass eigenstate \tilde{t}_1 via either $\tilde{t}_2 \rightarrow H\tilde{t}_1$ or $\tilde{t}_2 \rightarrow Z\tilde{t}_1$, followed in both cases by $\tilde{t}_1 \rightarrow t\tilde{\chi}_1^0$, where $\tilde{\chi}_1^0$ is an undetected, stable, lightest supersymmetric particle. The interpretation is performed in the region where the mass difference between the \tilde{t}_1 and $\tilde{\chi}_1^0$ states is approximately equal to the top-quark mass ($m_{\tilde{t}_1} - m_{\tilde{\chi}_1^0} \simeq m_t$), which is not probed by searches for direct \tilde{t}_1 squark pair production. The analysis excludes top squarks with masses $m_{\tilde{t}_2} < 575 \text{ GeV}$ and $m_{\tilde{t}_1} < 400 \text{ GeV}$ at a 95% confidence level.

Published in Physics Letters B as doi:10.1016/j.physletb.2014.07.053.

1 Introduction

Supersymmetry (SUSY) with R-parity conservation [1] is an extension to the standard model (SM) that provides a candidate particle for dark matter and addresses the hierarchy problem [2–7]. The hierarchy problem originates in the spin-zero nature of the Higgs (H) boson, whose mass is subject to divergences from higher-order corrections. The leading divergent contribution from SM particles arises from the H boson coupling to the top quark. SUSY provides a possible means to stabilize the H boson mass calculation, through the addition of contributions from a scalar top quark (top-squark) with a mass not too different from that of the top quark [8–12]. Searches for direct top-squark production from the ATLAS [13–18] and Compact Muon Solenoid (CMS) [19] Collaborations at the Large Hadron Collider (LHC) at CERN have focused mainly on the simplest scenario, in which only the lighter top-squark mass eigenstate, \tilde{t}_1 , is accessible at current LHC collision energies. In these searches, the top-squark decay modes considered are those to a top quark and a neutralino, $\tilde{t}_1 \rightarrow t\tilde{\chi}_1^0 \rightarrow bW\tilde{\chi}_1^0$, or to a bottom quark and a chargino, $\tilde{t}_1 \rightarrow b\tilde{\chi}_1^\pm \rightarrow bW\tilde{\chi}_1^\pm$. These two decay modes are expected to have large branching fractions if kinematically allowed. The lightest neutralino, $\tilde{\chi}_1^0$, is the lightest SUSY particle (LSP) in the R-parity conserving models considered; the experimental signature of such a particle is missing transverse energy (E_T^{miss}).

Searches for top-squark pair production are challenging because the cross section is approximately six times smaller than that for top-antitop quark pair ($t\bar{t}$) production if $m_{\tilde{t}_1} \sim m_t$ and decreases rapidly with increasing top-squark mass [20]. When the mass difference between the top-squark and the $\tilde{\chi}_1^0$ is large, top-squark production can be distinguished from $t\bar{t}$ production, as the former is typically characterized by events with extreme kinematic features, especially large E_T^{miss} . This strategy is being pursued in existing searches and has sensitivity to top-squark masses up to about 650 GeV for low $\tilde{\chi}_1^0$ masses [13–19]. The sensitivity of searches for direct top-squark pair production is, however, significantly reduced in the $\tilde{t}_1 \rightarrow t\tilde{\chi}_1^0$ decay mode for the region of SUSY parameter space in which $m_{\tilde{t}_1} - m_{\tilde{\chi}_1^0} \simeq m_t$. For example, in Ref. [19], the region $|m_{\tilde{t}_1} - m_{\tilde{\chi}_1^0} - m_t| \lesssim 20$ GeV is unexplored. In this region, the momentum of the daughter neutralino in the rest frame of the decaying \tilde{t}_1 is small, and it is exactly zero in the limit $m_{\tilde{t}_1} - m_{\tilde{\chi}_1^0} = m_t$. As a result, the E_T^{miss} from the vector sum of the transverse momenta of the two neutralinos is typically also small in the laboratory frame. It then becomes difficult to distinguish kinematically between \tilde{t}_1 pair production and the dominant background, which arises from $t\bar{t}$ production. This region of phase space can be explored using events with topologies that are distinct from the $t\bar{t}$ background. An example is gluino pair production where each gluino decays to a top squark and a top quark, giving rise to a signature with four top quarks in the final state [21, 22].

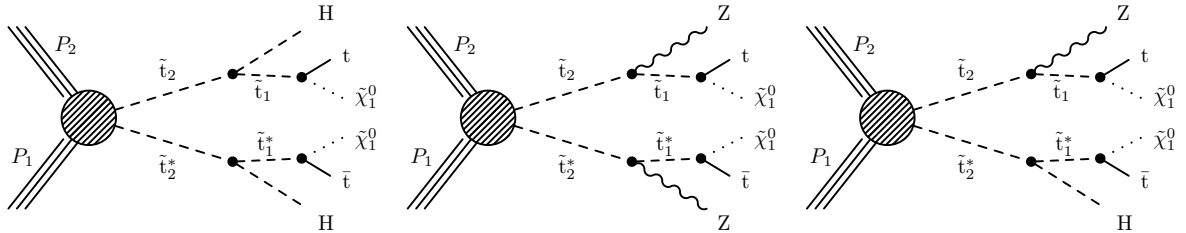


Figure 1: Diagrams for the production of the heavier top-squark (\tilde{t}_2) pairs followed by the decays $\tilde{t}_2 \rightarrow H\tilde{t}_1$ or $\tilde{t}_2 \rightarrow Z\tilde{t}_1$ with $\tilde{t}_1 \rightarrow t\tilde{\chi}_1^0$. The symbol * denotes charge conjugation.

This analysis targets the region of phase space where $m_{\tilde{t}_1} - m_{\tilde{\chi}_1^0} \simeq m_t$ by focusing on signatures of $t\bar{t}HH$, $t\bar{t}HZ$, and $t\bar{t}ZZ$ with E_T^{miss} . These final states can arise from the pair production of the heavier top-squark mass eigenstate \tilde{t}_2 . There are two non-degenerate top-squark mass eigen-

states (\tilde{t}_2 and \tilde{t}_1) due to the mixing of the SUSY partners \tilde{t}_L and \tilde{t}_R of the right- and left-handed top quarks. The \tilde{t}_2 decays to \tilde{t}_1 and an H or Z boson, and the \tilde{t}_1 is subsequently assumed to decay to $t\tilde{\chi}_1^0$, as shown in Fig. 1. Other decay modes such as $\tilde{t}_1 \rightarrow b\tilde{\chi}_1^+ \rightarrow bW\tilde{\chi}_1^0$ are largely covered for $m_{\tilde{t}_1} - m_{\tilde{\chi}_1^0} \simeq m_t$ by existing analyses [19]. The final states pursued in this search can arise in other scenarios, such as $\tilde{t}_1 \rightarrow t\tilde{\chi}_2^0$, with $\tilde{\chi}_2^0 \rightarrow H\tilde{\chi}_1^0$ or $\tilde{\chi}_2^0 \rightarrow Z\tilde{\chi}_1^0$. The analysis is also sensitive to a range of models in which the LSP is a gravitino [23, 24]. The relative branching fractions for modes with the H and Z bosons are model dependent, so it is useful to search for both decay modes simultaneously. In the signal model considered, \tilde{t}_2 is assumed always to decay to \tilde{t}_1 in association with an H or Z boson, such that the sum of the two branching fractions is $\mathcal{B}(\tilde{t}_2 \rightarrow H\tilde{t}_1) + \mathcal{B}(\tilde{t}_2 \rightarrow Z\tilde{t}_1) = 100\%$. Other possible decay modes are $\tilde{t}_2 \rightarrow t\tilde{\chi}_1^0$ and $\tilde{t}_2 \rightarrow b\tilde{\chi}_1^+$. These alternative decay modes are not considered here, since they give rise to final states that are covered by existing searches for direct top-squark pair production [13–19].

The results are based on proton-proton collision data collected at $\sqrt{s} = 8$ TeV by the CMS experiment at the LHC during 2012, corresponding to an integrated luminosity of 19.5 fb^{-1} . The analysis presented here searches for \tilde{t}_2 production in a sample of events with charged leptons, denoted by ℓ (electrons or muons), and jets identified as originating from bottom quarks (b jets). The four main search channels contain either exactly one lepton, two leptons with opposite-sign (OS) charge and no other leptons, two leptons with same-sign (SS) charge and no other leptons, or at least three leptons (3 ℓ). The channels with one lepton or two OS leptons require at least three b jets, while the channels with two SS leptons or 3 ℓ require at least one b jet. These requirements suppress background contributions from $t\bar{t}$ pair production, which has two b quarks and either one lepton or two OS leptons from the $t\bar{t} \rightarrow \ell\nu q\bar{q}b\bar{b}$ or $t\bar{t} \rightarrow \ell\nu\ell\nu b\bar{b}$ decay modes, where q denotes a quark jet. The sensitivity to the signal arises both from events with additional b quarks in the final state (mainly from $H \rightarrow b\bar{b}$), and from events with additional leptons from H or Z boson decays.

This letter is organized as follows: Section 2 briefly introduces the CMS detector, while Section 3 presents the event samples and the object selections used. Section 4 describes the signal regions, and Section 5 details the background estimation methods. The experimental results are presented in Section 6, and in Section 7 we discuss the interpretation of the results in the context of the signal model of the pair production of a heavier top-squark mass eigenstate \tilde{t}_2 decaying to a lighter top-squark mass eigenstate \tilde{t}_1 .

2 The CMS detector

The CMS detector [25] comprises a silicon tracker surrounded by a lead-tungstate crystal electromagnetic calorimeter and a brass-scintillator hadronic calorimeter, a superconducting solenoid supplying a 3.8 T magnetic field to the detectors enclosed, and a muon system. The silicon tracker system consists of pixel and strip detectors, which measure the trajectories of charged particles. Energy measurements of electrons, photons, and hadronic jets are provided by the electromagnetic and hadronic calorimeters. Each of these systems includes both central (barrel) and forward (endcap) subsystems. These detectors operate in the axial magnetic field of the solenoid, while muons are identified in gas-ionization detectors that are embedded in the steel flux-return yoke of the solenoid.

The CMS experiment uses a right-handed coordinate system with the origin at the nominal pp interaction point at the center of the detector. The positive x axis is defined by the direction from the interaction point to the center of the LHC ring, with the positive y axis pointing upwards. The azimuthal angle ϕ is measured around the beam axis in radians and the polar angle θ is

measured from the z axis pointing in the direction of the counterclockwise LHC beam. The pseudorapidity is defined as $\eta \equiv -\ln[\tan(\theta/2)]$.

The silicon tracker, the muon system, and the electromagnetic calorimeter cover the regions $|\eta| < 2.4$, $|\eta| < 2.4$, and $|\eta| < 2.5$, respectively. The hadronic calorimeters extend up to $|\eta| \approx 5$, improving momentum balance measurements in the plane transverse to the beam direction. The online trigger system that selects collision events of interest is based on two stages: a first-level hardware-based selection and a second set of requirements implemented in software.

3 Event samples, object selection, and event simulation

The data used for this search were collected with a high transverse-momentum (p_T) electron (e) or muon (μ) single-lepton trigger, which requires at least one electron with $p_T > 27\text{ GeV}$ or muon with $p_T > 24\text{ GeV}$. The trigger efficiencies, as measured with a sample of $Z \rightarrow \ell^+\ell^-$ events, vary between 85% and 97% for electrons, and between 80% and 95% for muons, depending on the η and p_T values of the leptons. Events were also collected with the ee, e μ , and $\mu\mu$ double-lepton triggers, which require at least one e or one μ with $p_T > 17\text{ GeV}$ and another with $p_T > 8\text{ GeV}$. Events are also acquired with a double-lepton trigger targeting lower- p_T leptons, requiring $p_T > 8\text{ GeV}$, but with an additional online selection of $H_T \equiv \sum_{\text{jet}} |p_T^{\text{jet}}| > 175\text{ GeV}$, considering only jets with $p_T > 40\text{ GeV}$ in the sum. The efficiencies lie between 90% and 95% for the trigger targeting lower- p_T leptons, and between 80% and 95% for the trigger targeting higher- p_T leptons, depending on the η and p_T values of the lower- p_T lepton. For selections with more than two leptons, the triggers are fully efficient.

Events are reconstructed offline using the particle-flow (PF) algorithm [26, 27]. Electron candidates are reconstructed by associating tracks with energy clusters in the electromagnetic calorimeter [28, 29]. Muon candidates are reconstructed by combining information from the tracker and the muon detectors [30]. Signal leptons are produced in the decays of W and Z bosons. In order to distinguish these leptons from those produced in the decays of heavy-flavor hadrons, all lepton candidates are required to be consistent with originating from the primary interaction vertex, chosen as the vertex with the highest sum of the p_T^2 of its constituent tracks. In particular they are required to have a transverse impact parameter with respect to this vertex smaller than 0.2 mm. A tighter requirement is used for the event category with two SS leptons (see Ref. [31]). Furthermore, since misidentified lepton candidates arising from background sources, such as the decays of hadrons, are typically embedded in jets, all lepton candidates are required to be isolated from hadronic activity in the event. This is achieved by imposing a maximum allowed value on the quantity p_T^{sum} , defined as the scalar sum of the p_T values of charged and neutral hadrons and photons within a cone of radius $\Delta R \equiv \sqrt{(\Delta\eta)^2 + (\Delta\phi)^2} = 0.3$ around the lepton candidate momentum direction at the origin. For the event category with at least three leptons, the isolation requirement is $p_T^{\text{sum}} < 0.15p_T$. For the lower lepton-multiplicity selections, the isolation requirement is tighter (see Refs. [19] and [31] for details). The surrounding hadronic activity is corrected for the energy contribution from additional proton-proton interactions in the event (pileup), as described in Ref. [32].

Jets are reconstructed from particle-flow candidates using the anti- k_T clustering algorithm [33] with a distance parameter of 0.5. Their energies are corrected for residual non-uniformity and non-linearity of the detector response using corrections derived from exclusive dijet and $\gamma/Z + \text{jet}$ data [34]. The energy contribution from pileup is estimated using the jet area method for each event [35] and is subtracted from the jet p_T . Only high- p_T jets in the central calorimeter $|\eta| < 2.4$ are considered. Jets consistent with the decay of heavy-flavor hadrons are identified

using the combined secondary vertex b-tagging algorithm at the medium or loose working points, defined such that they have tagging efficiencies of 70% or 80–85%, and misidentification rates for light-flavor jets less than 2% or 10%, respectively [36]. The E_T^{miss} is calculated as the magnitude of the vector sum of the transverse momenta of all PF candidates, incorporating jet energy corrections [37]. Quality requirements are applied to remove a small fraction of events in which detector effects such as electronic noise can affect the E_T^{miss} reconstruction. Events are required to have $E_T^{\text{miss}} > 50 \text{ GeV}$ to reduce background contributions from sources with a single W boson and from jet production via QCD processes.

Simulated event samples are used to study the characteristics of the signal and to calculate its acceptance, as well as for part of the SM background estimation. Pair production of \tilde{t}_2 squarks is described by the MADGRAPH 5.1.3.30 [38] program, including up to two additional partons at the matrix element level, which are matched to the parton showering from the PYTHIA 6.424 [39] program. The SUSY particle decays are simulated with PYTHIA with a uniform amplitude over phase space, so that all decays are isotropic [40]. The first two decay modes considered (see Fig. 1) are assumed to have a branching fraction of unity when setting limits on SUSY particle masses. The Higgs boson mass is set to 125 GeV [41], and its branching fractions are set according to the corresponding expectations from the SM [42]. For each decay mode, a grid of signal events is generated as a function of the two top-squark masses $m_{\tilde{t}_2}$ and $m_{\tilde{t}_1}$. The \tilde{t}_1 squark is forced to decay to a top quark and a neutralino LSP assuming $m_{\tilde{t}_1} - m_{\tilde{\chi}_1^0} = 175 \text{ GeV}$. The top-quark mass is set to 175 GeV. The signal event rates are normalized to cross sections calculated at next-to-leading order (NLO) in the strong coupling constant, including the resummation of soft-gluon emission at next-to-leading-logarithmic accuracy (NLO+NLL) [43–48].

The SM background processes considered are the production of $t\bar{t}$; $t\bar{t}$ in association with a boson (H , W , Z , γ^*); W , Z , and γ^* +jets; triboson; diboson; single-top quark in the s , t , and tW channels; and single-top quark in association with an additional quark and a Z boson. These processes are generated with the MADGRAPH, POWHEG-box 1.0 [49, 50], or MC@NLO 2.0.0 beta3 [51, 52] programs, using the CT10 [53] (POWHEG), CTEQ6M [54] (MC@NLO), and CTEQ6L1 [54] (MADGRAPH) parton distribution functions (PDFs). SM background event rates are normalized to cross sections [51, 52, 55–60] calculated at next-to-next-to-leading order when available, otherwise at NLO. All the background samples are processed with the full simulation of the CMS detector based on GEANT4 [61], while the generated signal samples use a fast simulation [62]. The fast simulation is validated against the full simulation for the variables relevant for this search, and efficiency corrections based on data are applied [63]. The simulation is generated with inelastic collisions superimposed on the hard-scattering event. Events are weighted so that the distribution of the number of inelastic collisions per bunch crossing matches that in data.

4 Event categories and signal regions

The search is carried out through comparisons of the data and SM background yields in disjoint signal regions (SRs) targeting the SUSY processes shown in Fig. 1, while suppressing the contributions from SM backgrounds, predominantly $t\bar{t}$ production. The definitions of the SRs are summarized in Table 1, and are detailed in the following subsections. Events are classified according to the lepton multiplicity and charge requirements on the leptons. Four main event categories are considered. The first two include events with one lepton or two OS leptons. Since these lepton signatures also arise in the decays of top-antitop quark pairs, requirements of at least three b jets are used to suppress this background. The other two categories are events with exactly two SS leptons and events with three or more leptons, which do not typically arise

in $t\bar{t}$ events. A requirement of at least one b jet is applied to further suppress the contribution from backgrounds from W and Z bosons. Lepton vetoes are used to ensure that the four main event categories do not overlap.

Table 1: Summary of the SR definitions for the different selections, specified by rows in the table. The SRs correspond to all possible combinations of requirements in each row, where different regions for the kinematic variables are separated by commas. For the event category with two SS leptons, two selections in lepton p_T are used (low and high), as explained in the text. There are 96 SRs in total.

N_ℓ	Veto	N_b jets	N_{jets}	E_T^{miss} [GeV]	Additional requirements [GeV]
1	track or τ_h	=3	≥ 5	≥ 50	$m_T > 150$ $m_T > 120$
		≥ 4	≥ 4		
2 OS	extra e/ μ	= 3	≥ 5	≥ 50	$N_{bb} = 1$ with $100 \leq m_{bb} \leq 150$ or $N_{bb} \geq 2$
		≥ 4	≥ 4		
2 SS	extra e/ μ	≥ 1 ≥ 2	[2, 3], ≥ 4	[50, 120], ≥ 120	for low (high) p_T : $250(200) \leq H_T \leq 400$, $H_T \geq 400$
≥ 3	—	= 1	[2, 3], ≥ 4	[50, 100], [100, 200], ≥ 200	for on/off-Z: $60 \leq H_T \leq 200$, $H_T \geq 200$
		= 2	≥ 4		
		≥ 3	≥ 3		

4.1 Event categories with a single lepton or two opposite-sign leptons

The event categories with one lepton or two OS leptons, accompanied in either case by at least three b jets, target signatures with H bosons, which have large branching fraction for $H \rightarrow b\bar{b}$. In the single-lepton channel, events are required to have exactly one electron with $p_T > 30$ GeV and $|\eta| < 1.44$ or exactly one muon with $p_T > 25$ GeV and $|\eta| < 2.1$. Events with an indication of an additional lepton, either an isolated track [31] or a hadronically decaying τ -lepton candidate τ_h [64–66], are rejected in order to reduce the background from $t\bar{t}$ events in which both W bosons decay leptonically. In the double-lepton channel, events are required to contain exactly two charged leptons (ee, e μ , or $\mu\mu$), each with $p_T > 20$ GeV and $|\eta| < 2.4$. In this case, events with an additional e or μ with $p_T > 10$ GeV are rejected. Any electron candidate in the region $1.44 < |\eta| < 1.57$, a less well-instrumented transition region between the barrel and endcap regions of the calorimeter, is excluded in the event selection since standard electron identification capabilities are not optimal. Jets are required to be separated from the candidate leptons by $\Delta R > 0.4$.

In these event categories, a typical $t\bar{t}$ background event has two b jets in the final state, while signal events could have up to four additional b jets, two from each H decay. The requirement of more than two b jets greatly suppresses the $t\bar{t}$ background contribution. For events with exactly three b jets, the jet p_T threshold applied is 40 GeV; for events with at least four b jets, the threshold is lowered to 30 GeV. In both cases, the medium working point of the b-jet tagger is used (see Section 3). To further reduce the $t\bar{t}$ background contribution in the sample with exactly three b jets, events are required to contain two additional jets with $p_T > 30$ GeV, at least one of which must satisfy the loose but not the medium criteria of the b-jet tagger. Signal events can have large jet and b-jet multiplicities, while in the case of the $t\bar{t}$ background, additional jets are needed to satisfy this selection criterion. To reduce the contribution of jets from pileup in the event, a requirement is applied on a multivariate discriminating variable that incorporates the multiplicity of objects clustered in the jet, the jet shape, and the compatibility of the charged constituents of the jet with the primary interaction vertex [67].

Besides the requirements listed above, the analysis in the single-lepton channel selects events with large transverse mass of the (ℓ, ν) system, defined as $m_T \equiv \sqrt{2p_T^\ell p_T^\nu [1 - \cos(\phi^\ell - \phi^\nu)]}$,

where the p_T of the selected lepton is used and the (x, y) components of the neutrino momentum are equated to the corresponding E_T^{miss} components. For events in which the E_T^{miss} arises from a single neutrino from a W boson decay, this variable has a kinematic endpoint $m_T \approx m_W$, where m_W is the W boson mass. The requirement of large m_T ($m_T > 150 \text{ GeV}$ for events with three b jets or $m_T > 120 \text{ GeV}$ for events with at least four b jets) provides strong suppression of the semileptonic $t\bar{t}$ background.

The study of the OS dilepton channel uses information from pairs of b jets (ignoring their charge) to identify pairs consistent with $H \rightarrow bb$ decay: $\Delta R_{bb} \leq 2\pi/3$, $m_{bb}/[p_T^{bb}\Delta R_{bb}] \leq 0.65$, and $|\Delta y_{bb}| \leq 1.2$, where the rapidity is defined as $y \equiv \frac{1}{2} \ln[(E + p_z)/(E - p_z)]$, with p_z denoting the component of the momentum along the beam axis. Only b jets satisfying the medium working point of the tagger are used to form bb combinations. Different b-jet pairs are not allowed to have b-jets in common. We denote the number of selected b-jet pairs as N_{bb} and the invariant mass of a pair as m_{bb} . Events are required to have either $N_{bb} = 1$ and $100 \leq m_{bb} \leq 150 \text{ GeV}$, or else $N_{bb} \geq 2$. For the signal models of interest, particularly the $\tilde{t}_2 \rightarrow H\tilde{t}_1$ decay mode, the SRs with largest b-jet multiplicity (≥ 4 b jets) have the highest sensitivity.

4.2 Event category with two SS leptons

The event category with two SS leptons targets signatures with multiple sources of leptons. Standard model processes with two SS leptons are extremely rare. The analysis for this event category closely follows that described in Ref. [31]. The only difference is the addition of a veto on events containing a third lepton, to remove the overlap with the 3ℓ event category. These SRs also recover events with three leptons in which one of the three leptons falls outside the detector acceptance or fails the selection criteria. Multiple SRs are defined for the SS event category based on the jet and b-jet multiplicities, E_T^{miss} , and H_T , and on whether the leptons satisfy $p_T > 10 \text{ GeV}$ (low- p_T analysis) or $p_T > 20 \text{ GeV}$ (high- p_T analysis). The leptons must appear within $|\eta| < 2.4$. The jet p_T threshold applied is 40 GeV . The low and high lepton p_T samples, which partially overlap, target complementary signatures. The low- p_T sample extends the sensitivity to signatures with compressed SUSY spectra, while the high- p_T analysis targets scenarios with leptons produced via on-shell W and Z bosons. Only the high- p_T analysis is used to target the signals explicitly studied in this letter, while the low- p_T analysis is included for sensitivity to other new physics scenarios.

4.3 Event category with at least three leptons

The event category with at least three leptons and at least one b jet is sensitive to all of the processes shown in Fig. 1. These processes contain many sources of leptons, such as Z bosons from the top-squark decays, and τ leptons and W and Z bosons from the H boson decays. Even though signatures giving rise to three or more leptons have small production rates, this event category has good sensitivity because the backgrounds are strongly suppressed. The dataset is acquired using the double-lepton triggers. Events are selected offline by requiring at least three e or μ candidates with $p_T > 10 \text{ GeV}$, including at least one with $p_T > 20 \text{ GeV}$, and $|\eta| < 2.4$. Events with two leptons of opposite-sign charge with an invariant mass below 12 GeV are removed from the sample to reduce the contribution of leptons originating from low-mass bound states.

Events are required to have at least two jets with $p_T > 30 \text{ GeV}$ and at least one b jet satisfying the medium working point of the tagger. Leptons within $\Delta R < 0.4$ of a b-quark jet are not considered isolated and are merged with the b jet. This requirement imposes an additional isolation criterion for leptons and reduces the dominant background, $t\bar{t}$ production, by 25–40% depending on the SR, compared to the case where such an object is reconstructed as a lepton

rather than a b jet. The efficiency for signal leptons is reduced by 1%. The remaining SM background in the $\geq 3 \ell$ event category from WZ+jets production is highly suppressed by the b-jet requirement.

This three-lepton event sample is divided into several SRs by imposing requirements on the jet and b jet multiplicity, E_T^{miss} , and the hadronic activity in the event, as given by the kinematic variable H_T , considering jets with $p_T > 30 \text{ GeV}$ in the sum. Finally, events are classified as either “on-Z” if there is a pair of leptons with the same flavor and opposite charge that has an invariant mass within 15 GeV of the nominal Z boson mass, or “off-Z” if no such pair exists or if the invariant mass lies outside this range.

The separation of events into these SRs improves the sensitivity of the search. For the signal models of interest, the SRs with large b jet multiplicity (those designated $N_{\text{b jets}} = 2$ and $N_{\text{b jets}} \geq 3$) and that with both high E_T^{miss} and high H_T provide the greatest sensitivity. The on-Z regions are the most sensitive, when the decay to an on-shell Z boson is kinematically allowed for the $\tilde{t}_2 \rightarrow Z \tilde{t}_1$ decay mode. Conversely, the off-Z regions have more sensitivity when on-shell Z boson decays are not kinematically allowed and for the $\tilde{t}_2 \rightarrow H \tilde{t}_1$ decay mode.

5 Background estimation

The main background arises from SM $t\bar{t}$ events, which usually have two b jets and at most two leptons from W boson decays. Thus, $t\bar{t}$ events can only satisfy the selection criteria if accompanied by sources of additional b jets or leptons. Such backgrounds are estimated using control samples in data, as described below. This method greatly reduces the dependence of the background prediction on the accurate modeling in simulation, the knowledge of the inclusive $t\bar{t}$ production cross-section, the measurement of the integrated luminosity, and the accuracy of the object-selection efficiency determination.

Additional backgrounds arise from processes involving one or more W and Z bosons, although these contributions are suppressed by the b-jet requirements. Finally, all event categories have backgrounds from rare SM processes, such as $t\bar{t}Z$ and $t\bar{t}W$ production, whose cross sections have not been precisely measured [68]. The prediction for these contributions is derived from simulation, and a systematic uncertainty of 50% is assigned to account for the uncertainty in the NLO calculations of their differential cross sections. The remainder of this section describes the background predictions for each of the specific event categories.

5.1 Backgrounds in event categories with a single lepton or two OS leptons

For the single-lepton or two-OS-lepton event categories, the dominant background is from $t\bar{t}$ events (85–95% of the total). These events can have three or more b jets if the $t\bar{t}$ pair is accompanied by additional jets that may be mistagged in the case of light-parton jets or that may contain genuine b jets from gluon decays to a bb pairs. In the case of semileptonic $t\bar{t}$ events, there are small additional contributions from $W \rightarrow c\bar{s}$ decays, with a charm-quark jet misidentified as a b jet, and from the rare $W \rightarrow c\bar{b}$ decay mode. In the case of dileptonic $t\bar{t}$ events, τ leptons from the second W boson decay that are misidentified as b jets also contribute. Scale factors, defined as the ratio of the yield in data to the yield in simulation, are used to normalize the background predictions from simulation. For each SR, the corresponding scale factor is derived from a control region enhanced in background $t\bar{t}$ events. These control regions are defined by $50 \leq m_T \leq 100 \text{ GeV}$ for the single-lepton selections and by either $N_{bb} = 0$ or $N_{bb} = 1$, with either $m_{bb} \leq 100 \text{ GeV}$ or $m_{bb} \geq 150 \text{ GeV}$, for the OS-dilepton case. The contribution from non- $t\bar{t}$ events is evaluated from simulation and subtracted from the data before deriving the normal-

ization. To reduce the contribution from a possible signal in these control regions, the samples are restricted to events with low jet multiplicity: for the three-b-jet category, only events with exactly five jets are used, and for the category with four b jets, only events with exactly four jets are used. The dominant source of uncertainty for the background prediction arises from the limited number of events in the control samples (15–35% on the total background). The $t\bar{t}$ background prediction also depends on the ratio of events in the signal and control regions, which is evaluated from simulation and validated using $t\bar{t}$ -dominated control samples obtained by selecting events with fewer than three b jets, as described below.

In the single-lepton channel, the modeling of the high- m_T tail is critical for the background estimation. Genuine semileptonic $t\bar{t}$ events have an endpoint at $m_T \approx m_W$, with E_T^{miss} resolution effects primarily responsible for populating the $m_T > m_W$ tail. The effect of E_T^{miss} resolution on the m_T tails is investigated by selecting events with one or two b jets and by varying the number of additional jets. The comparison of simulation with data in the m_T tail region is used to extract scale factors and uncertainties for the semileptonic $t\bar{t}$ prediction. The scale factors are in the range 1.1–1.2, depending on the m_T requirement, with corresponding uncertainties of 5–10%. The semileptonic background contributes 50–60% of the total background in the single-lepton SRs. Events from genuine dileptonic $t\bar{t}$ events can also satisfy the single-lepton event selection if the second lepton is not identified or is not isolated and can give rise to large values of E_T^{miss} and m_T due to the presence of two neutrinos. This $t\bar{t} \rightarrow \ell\ell + \text{jets}$ contribution constitutes ∼30–40% of the total background and is derived from simulation, with scale factors consistent with unity, as determined from comparison of data with simulation in the dilepton control regions.

In the channels with two OS leptons, the most important issues for the background prediction are related to the construction of b-jet pairs (see Section 4.1 for the full list of requirements). Modeling of the emission of additional radiation leading to jets and gluon splitting to $b\bar{b}$ pairs, and of effects such as τ -lepton mistagging, c-quark-jet mistagging, and b-jet identification efficiency, can affect the m_{bb} variable. The modeling of these effects is validated using the statistically precise single-lepton control sample with $50 \leq m_T \leq 100$ GeV, in which the m_{bb} distributions in data and simulation are compared as a function of the b-jet multiplicity. The ratio of the number of events satisfying the N_{bb} and m_{bb} requirements that define the signal and control regions is compared in data and simulation. This study is used to derive scale factors, which are found to be consistent with unity, and uncertainties corresponding to 20–30% of the total background uncertainty.

5.2 Backgrounds in the event category with two SS leptons

For the SRs with two SS leptons, the background estimates and uncertainties are derived following the procedures described in Ref. [31]. There are three main categories of backgrounds. Non-prompt leptons are produced from heavy-flavor decays, misidentified hadrons, muons from the decay-in-flight of light mesons, and electrons from unidentified photon conversions. Charge misidentification arises mainly from electrons that undergo severe bremsstrahlung in the tracker material, leading to a misreconstruction of the charge sign. Finally, rare SM processes yielding two genuine SS leptons (typically a $t\bar{t}$ pair in association with an H, W, or Z boson) can contribute significantly, especially in SRs with tight selection requirements. Backgrounds from non-prompt leptons and rare SM processes dominate, each contributing 20–80% of the total, while charge misidentification contributes 1–5%.

The background from non-prompt leptons is evaluated using the event yield in a control sample in which the same analysis selections are applied, except there is at least one lepton that

passes a loose lepton selection but fails the full set of tight identification and isolation requirements. This observed yield is corrected by a “tight-to-loose” ratio, the probability that a loosely identified non-prompt lepton also passes the full set of requirements. This correction factor is in turn measured in a control sample of QCD multijet events enriched in non-prompt leptons. The ratio is obtained as a function of lepton p_T and η . The event kinematics and the various sources of non-prompt leptons are different in the QCD multijet sample, where the tight-to-loose ratio is measured, and the signal sample, where it is applied. This gives rise to a systematic uncertainty in the non-prompt lepton background estimate. The charge misidentification background is obtained using a sample of OS ee and $e\mu$ events that satisfy the full kinematic selection weighted by the p_T - and η -dependent probability of electron charge misassignment. The systematic uncertainty of the total background prediction is dominated by the uncertainties from rare SM processes and from events with a jet misidentified as a prompt lepton (30–50% of the total background).

5.3 Backgrounds in the event category with at least three leptons

For SRs with at least three leptons, there are two main types of backgrounds. In the off-Z SRs, the background with two prompt leptons and an additional object misidentified as a prompt lepton dominates, comprising 50–90% of the total. In the on-Z SRs, the dominant background is typically from SM processes with at least three genuine prompt leptons, corresponding to 60–100% of the total.

The background sources with two prompt leptons from W or Z boson decay and a third object misidentified as a prompt lepton are predominantly from $t\bar{t}$ production, although the Z + jets and WW + jets processes also contribute. The procedure to estimate this background contribution follows closely that used for the analysis of events with two SS leptons [31]. The probability for a loosely identified lepton to satisfy the full set of selection requirements is applied to a sample of $\geq 3 \ell$ events, in which the isolation requirement on one of the leptons is removed, providing an estimate of the background contribution from non-prompt leptons. A systematic uncertainty of 30% is derived for this background based on studies of the method in simulation. This uncertainty accounts for the difference in the p_T spectrum of b jets in the control sample, where the probability is measured, compared to the spectrum in the signal sample, where it is applied. This systematic uncertainty dominates the uncertainty in the background prediction in the SRs with looser kinematic requirements. SRs with tight kinematic requirements also have a significant statistical uncertainty due to the size of the sample used to derive this background estimate. These are the dominant sources of uncertainty in the backgrounds in the off-Z signal regions, corresponding to 20–90% uncertainty on the total background.

The background contribution from events with two vector bosons that produce three genuine prompt isolated leptons, mainly WZ + jets and ZZ + jets events, is estimated from simulation and is validated by comparing data and simulation in control samples in which the full selection is applied and the b-jet requirement is inverted. A control sample enhanced in the WZ background is obtained by selecting events with three high- p_T leptons. One pair of leptons is required to form a $Z \rightarrow \ell^+\ell^-$ candidate. The third lepton is combined with the E_T^{miss} vector, and this system is required to form a W boson candidate ($50 < E_T^{\text{miss}} < 100 \text{ GeV}$ and $50 < m_T < 120 \text{ GeV}$). A second control sample, enhanced in the ZZ background, is obtained by selecting events with four leptons and $E_T^{\text{miss}} < 50 \text{ GeV}$. Two leptons are required to form a Z candidate. Scale factors are derived based on the comparison of data and simulation in these control samples. The scale factors are found to be unity and 0.9 for the WZ and ZZ backgrounds, respectively. The systematic uncertainty for the diboson background is derived based on these comparisons, which are limited by the statistical precision of the control samples. A

50% uncertainty is assigned to account for possible mismodeling of additional partons required to satisfy the b-jet requirement.

6 Results

The results of the search are shown in Tables 2-4, and in Figs. 2-4, where the background predictions are broken down into the various components.

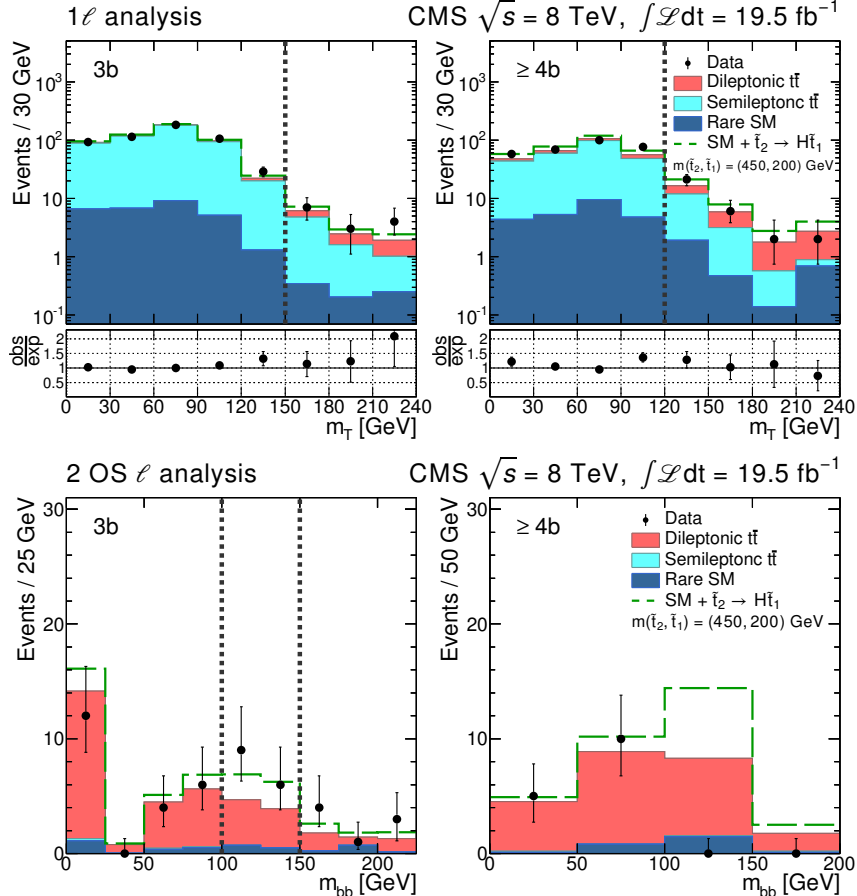


Figure 2: Comparison of the m_T distributions for events with one lepton (top row) and m_{bb} distributions for events with two OS leptons (bottom row) in data and MC simulation satisfying the 3b (left) and $\geq 4b$ (right) SR requirements. The vertical dashed lines indicate the corresponding signal region requirement. The semileptonic $t\bar{t}$ and dileptonic $t\bar{t}$ components represent simulated events characterized by the presence of one or two W bosons decaying to e, μ or τ . The yields of the $t\bar{t}$ simulated samples are adjusted so that the total SM prediction is normalized to the data in the samples obtained by inverting the SR requirements. The distribution for the model $\tilde{t}_2 \rightarrow H\tilde{t}_1$ where $m_{\tilde{t}_2} = 450$ GeV and $m_{\tilde{t}_1} = 200$ GeV is displayed on top of the backgrounds. The last bin contains the overflow events. The uncertainties in the background predictions are derived for the total yields in the signal regions and are listed in Table 2.

For the event selections with one lepton, Fig. 2 (top) shows a comparison of the m_T distribution in data and simulation. The sample at low m_T is enhanced in semileptonic $t\bar{t}$ events and is used as a control sample to derive the normalization for this background contribution. As shown in Fig. 2 (top), the backgrounds in the SR are mainly semileptonic and dileptonic $t\bar{t}$ events.

For the SRs with two OS leptons, Fig. 2 (bottom) shows a comparison of the m_{bb} distribution in

Table 2: Selection with one lepton or two OS leptons: background predictions and observed data yields. The uncertainties in the total background predictions include both the statistical and systematic components.

N_b jets	N_{jets}	$E_{\text{T}}^{\text{miss}}$ [GeV]	1 ℓ high m_{T}		2 OS ℓ and bb requirement	
			Bkg.	Obs.	Bkg.	Obs.
=3	≥ 5	≥ 50	10.0 ± 1.8	14	8.4 ± 2.7	15
≥ 4	≥ 4		27 ± 6	31	11 ± 5	3

data and simulation. The sample in the region outside the m_{bb} signal window is used to derive the normalization for the $t\bar{t} \rightarrow \ell\ell + \text{jets}$ background prediction for events with three b jets. In the case of events with at least four b jets, multiple bb pairs are possible. The control region is not indicated in Fig. 2 (bottom right) since the m_{bb} requirement is not applied when $N_{\text{bb}} \geq 2$.

The dominant background in the SRs is from $t\bar{t} \rightarrow \ell\ell + \text{jets}$ events. The results for the SRs with one lepton or two OS leptons are summarized in Table 2. The predicted and observed yields agree within 1.4 standard deviations of local significance [69], given the statistical uncertainty in the predicted yields.

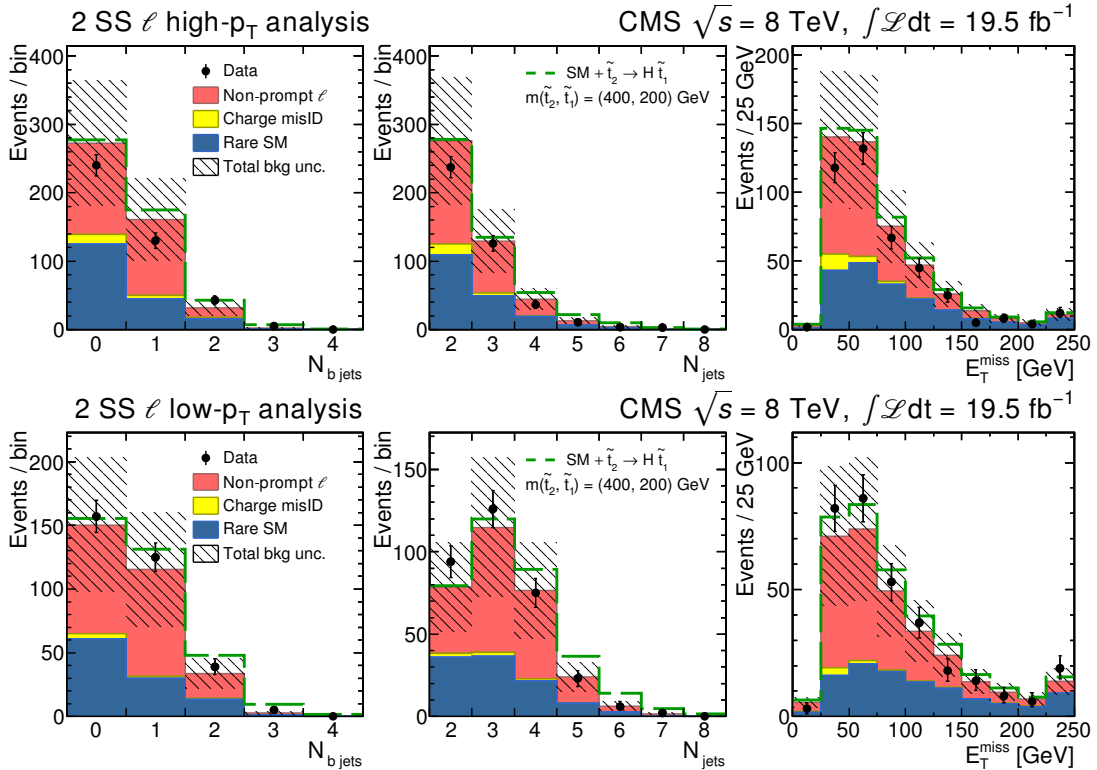


Figure 3: Data and predicted SM background for the event sample with two SS leptons as a function of number of b jets, number of jets, and $E_{\text{T}}^{\text{miss}}$ for events satisfying the high- p_{T} (top row) or the low- p_{T} (bottom row) selection. The shaded bands correspond to the total estimated uncertainty in the background prediction. The distribution for the model $\tilde{t}_2 \rightarrow H \tilde{t}_1$ where $m_{\tilde{t}_2} = 400$ GeV and $m_{\tilde{t}_1} = 200$ GeV is displayed on top of the backgrounds. The last bin in the histograms includes overflow events.

Figure 3 shows a comparison of data and the predicted backgrounds for events with two SS leptons satisfying a more inclusive selection, which is enhanced in SM processes: at least two jets, moderate H_{T} (> 250 GeV in the low- p_{T} analysis and > 80 GeV in the high- p_{T} analysis), and moderate $E_{\text{T}}^{\text{miss}}$ (> 30 GeV for events with $H_{\text{T}} < 500$ GeV; otherwise, there is no $E_{\text{T}}^{\text{miss}}$ require-

Table 3: SS dilepton event category: predicted total background and observed data yields as a function of the jet multiplicity, b-jet multiplicity, E_T^{miss} , and H_T requirements, for the low- p_T and high- p_T regions. The uncertainties in the total background predictions contain the statistical and systematic components.

Selection			low- p_T				high- p_T			
N_b jets	N_{jets}	E_T^{miss} [GeV]	$H_T \in [250, 400]$ GeV	$H_T \geq 400$ GeV	$H_T \in [200, 400]$ GeV	$H_T \geq 400$ GeV	$B_{\text{kg.}}$	$O_{\text{bs.}}$	$B_{\text{kg.}}$	$O_{\text{bs.}}$
$= 1$	2–3	50–120	29 ± 12	$39 \pm 5.6 \pm 2.0$	5	31 ± 12	$27 \pm 3.4 \pm 1.2$	5	3.4 ± 1.2	5
		≥ 120	11 ± 4	$8 \pm 4.9 \pm 1.8$	5	9.0 ± 3.2	$9 \pm 3.5 \pm 1.3$	2	3.5 ± 1.3	2
	≥ 4	50–120	15 ± 6	$15 \pm 10 \pm 4$	6	9.2 ± 3.4	$6 \pm 5.4 \pm 2.0$	2	5.4 ± 2.0	2
		≥ 120	3.9 ± 1.5	$3 \pm 6.1 \pm 2.2$	10	2.6 ± 1.0	$3 \pm 3.5 \pm 1.3$	6	3.5 ± 1.3	6
≥ 2	2–3	50–120	6.6 ± 2.4	$10 \pm 1.3 \pm 0.5$	1	6.0 ± 2.1	$11 \pm 0.78 \pm 0.34$	1	0.78 ± 0.34	1
		≥ 120	2.4 ± 0.9	$1 \pm 1.2 \pm 0.5$	2	2.4 ± 0.9	$3 \pm 0.8 \pm 0.4$	1	0.8 ± 0.4	1
	≥ 4	50–120	6.5 ± 2.5	$5 \pm 4.0 \pm 1.5$	11	3.4 ± 1.3	$2 \pm 2.3 \pm 1.0$	7	2.3 ± 1.0	7
		≥ 120	1.8 ± 0.7	$0 \pm 3.1 \pm 1.2$	3	1.1 ± 0.5	$0 \pm 2.0 \pm 0.8$	2	2.0 ± 0.8	2

ment). This sample serves to validate the methods used to predict the backgrounds in the SRs, which are defined by applying requirements on the selection observables shown: the jet multiplicity, the b-jet multiplicity, and E_T^{miss} , as well as H_T . The amount of background varies strongly among the signal regions; some of them including tens of background events while others have essentially none. The relative contribution from rare SM processes increases as the requirements are tightened. As shown in Table 3, the SM background predictions and observations in the SRs are in agreement for both the high- p_T and low- p_T selections.

Table 4: Predicted total background and observed data yields as a function of the jet multiplicity, b-jet multiplicity, E_T^{miss} , and H_T requirements, for events with at least three leptons, with (on-Z) and without (off-Z) a Z boson candidate present. The uncertainties in the total background predictions include both the statistical and systematic components.

Selection			off-Z				on-Z			
N_b jets	N_{jets}	E_T^{miss} [GeV]	$H_T \in [60, 200]$ GeV	$H_T \geq 200$ GeV	$H_T \in [60, 200]$ GeV	$H_T \geq 200$ GeV	$B_{\text{kg.}}$	$O_{\text{bs.}}$	$B_{\text{kg.}}$	$O_{\text{bs.}}$
$= 1$	2–3	50–100	34 ± 7	$36 \pm 11.2 \pm 2.5$	9	16 ± 5	$30 \pm 10 \pm 4$	13	10 ± 4	13
		100–200	12.2 ± 2.7	$13 \pm 9.1 \pm 2.1$	6	5.3 ± 1.8	$6 \pm 5.9 \pm 2.1$	3	5.9 ± 2.1	3
		≥ 200	0.33 ± 0.22	$0 \pm 1.2 \pm 0.5$	0	0.37 ± 0.23	$0 \pm 0.9 \pm 0.4$	0	0.9 ± 0.4	0
	≥ 4	50–100	0.9 ± 0.4	$2 \pm 5.4 \pm 1.3$	3	0.11 ± 0.13	$1 \pm 5.0 \pm 2.0$	4	5.0 ± 2.0	4
		100–200	0.10 ± 0.12	$0 \pm 3.6 \pm 1.0$	3	0.08 ± 0.12	$0 \pm 3.0 \pm 1.3$	5	3.0 ± 1.3	5
		≥ 200	0.0 ± 0.1	$0 \pm 0.76 \pm 0.35$	0	0.02 ± 0.10	$0 \pm 0.56 \pm 0.32$	1	0.56 ± 0.32	1
$= 2$	2–3	50–100	4.9 ± 1.2	$7 \pm 3.9 \pm 1.2$	7	2.4 ± 0.9	$5 \pm 2.5 \pm 1.1$	2	2.5 ± 1.1	2
		100–200	2.3 ± 0.7	$1 \pm 1.9 \pm 0.7$	0	1.3 ± 0.5	$1 \pm 1.4 \pm 0.6$	1	1.4 ± 0.6	1
		≥ 200	0.22 ± 0.21	$1 \pm 0.14 \pm 0.14$	0	0.12 ± 0.13	$0 \pm 0.43 \pm 0.26$	0	0.43 ± 0.26	0
	≥ 4	50–100	0.03 ± 0.11	$0 \pm 2.8 \pm 0.9$	1	0.20 ± 0.17	$1 \pm 2.9 \pm 1.3$	1	2.9 ± 1.3	1
		100–200	0.05 ± 0.11	$0 \pm 1.7 \pm 0.6$	0	0.10 ± 0.13	$0 \pm 1.7 \pm 0.8$	0	1.7 ± 0.8	0
		≥ 200	0.0 ± 0.1	$0 \pm 0.38 \pm 0.21$	0	0.0 ± 0.1	$0 \pm 0.29 \pm 0.19$	0	0.29 ± 0.19	0
≥ 3	≥ 3	50–100	0.0 ± 0.1	$0 \pm 0.56 \pm 0.27$	1	0.0 ± 0.1	$0 \pm 0.18 \pm 0.15$	0	0.18 ± 0.15	0
		100–200	0.02 ± 0.11	$0 \pm 0.18 \pm 0.14$	0	0.0 ± 0.1	$0 \pm 0.25 \pm 0.17$	0	0.25 ± 0.17	0
		≥ 200	0.0 ± 0.1	$0 \pm 0.2 \pm 0.2$	0	0.0 ± 0.1	$0 \pm 0.02 \pm 0.10$	0	0.02 ± 0.10	0

Finally, for the event sample with at least three leptons, Fig. 4 shows a comparison of data and the predicted backgrounds for the jet and b-jet multiplicities and for the E_T^{miss} distribution. The dominant background is from processes with two prompt leptons and additional non-prompt leptons, mainly due to $t\bar{t}$ events, although in the case of the on-Z selection, background sources with Z bosons also contribute significantly. The results of the search, summarized in Table 4, demonstrate agreement between background predictions and observations for all the SRs considered.

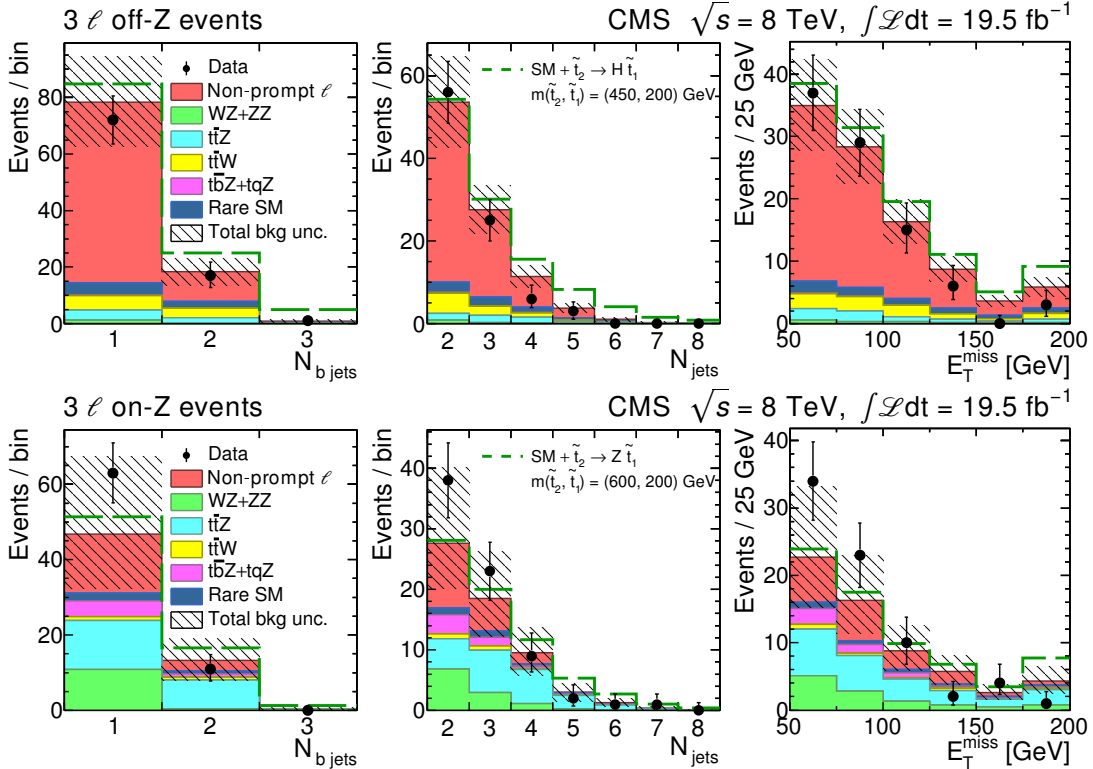


Figure 4: Data and predicted SM background for the event sample with at least three leptons as a function of number of b jets, number of jets, and E_T^{miss} for events that do not contain (off-Z), top row, or contain (on-Z), bottom row, an OS same-flavor pair that is a Z boson candidate. The shaded bands correspond to the total estimated uncertainty in the background prediction. The distributions for the models $\tilde{t}_2 \rightarrow H\tilde{t}_1$ and $\tilde{t}_2 \rightarrow Z\tilde{t}_1$ are displayed on top of the backgrounds in the top and bottom rows respectively. The top-squark masses are $m_{\tilde{t}_1} = 200$ GeV and $m_{\tilde{t}_2} = (450, 600)$ GeV for the (H, Z) channel. The last bin in the histograms includes overflow events.

In summary, the data yields are found to be consistent with the background predictions across all event categories and SRs. Of the 96 SRs, the largest discrepancy corresponds to a 1.6 standard deviation excess of local significance (30 events compared to 16 ± 5 expected, see Table 4), computed following the recommendations of Ref. [69]. Thus, no indication of top-squark pair production is observed.

7 Interpretation

The results are used to set upper limits on the cross section times branching fraction for pair production of \tilde{t}_2 squarks for the decay modes shown in Fig. 1. The upper limits are calculated at a 95% confidence level (CL) using the LHC-style CL_S method [70–72]. The exclusion curves on particle masses at 95% CL are evaluated from a comparison of the cross section upper limits and the theoretical signal cross section predictions. As explained below, the results from the various SRs are combined in the limit-setting procedure in order to improve the sensitivity of the search.

The limit calculation on the cross section times branching fraction depends on the signal selection efficiency and the background estimates. The SRs with at least three leptons have the highest expected sensitivity because of the small level of SM background. For SRs with at least three leptons, the off-Z SRs with $H_T > 200$ GeV are used for the $t\bar{t}HH$ interpretation, while

both the off-Z and on-Z SRs with $H_T > 200 \text{ GeV}$ are used for the $t\bar{t}ZZ$ interpretation. The total signal acceptance for all SRs with at least three leptons varies from around 0.4–0.5% for the $t\bar{t}HH$ signal, to 1.2–1.5% for the $t\bar{t}ZZ$ signal. The acceptance for the most sensitive SR alone is around $\sim 0.1\%$ for $t\bar{t}HH$ and approximately three times larger for $t\bar{t}ZZ$. This difference in acceptance is due to the larger leptonic branching fraction for Z boson decays compared to H boson decays. The SRs with lower lepton multiplicities also have sensitivity to the $t\bar{t}HH$ signal. All SRs of the high- p_T SS dilepton analysis are used in the limit setting. While only the high- p_T results are used in the interpretation presented in this letter, the low- p_T experimental results are included in Table 3 for potential use in future interpretations. In SRs with two SS leptons, the overall acceptance for $t\bar{t}HH$ events is 0.3–0.5%, where the most sensitive signal regions contribute $\sim 0.15\%$. In the case of SRs with one lepton or two OS leptons, the acceptance for $t\bar{t}HH$ events is approximately 0.2–0.4%. The acceptances for the single-lepton and dilepton final states are slightly lower for the $t\bar{t}ZZ$ signal. Because of the large branching fraction for the $H \rightarrow b\bar{b}$ decay mode, SRs with higher b-jet multiplicity requirements dominate the expected sensitivity for scenarios with H bosons. SRs with low b-jet multiplicities are most sensitive for scenarios with Z bosons.

The systematic uncertainties, listed in Table 5, are evaluated for the signal selection efficiency in every SR and for every signal point separately. The total uncertainty in the signal selection efficiency is in the 9–30% range. The dominant source of uncertainty depends on the SR and decay mode considered. An important source of uncertainty arises from the estimation of the trigger and lepton identification efficiencies, which are derived using $Z \rightarrow \ell^+\ell^-$ samples and contribute 6–13%. The uncertainty due to the knowledge of the energy scale of hadronic jets increases with tighter kinematic requirements and corresponds to an uncertainty of 1–15%. The uncertainty due to the knowledge of the b jet identification performance depends on the event properties, such as the jet flavor and p_T value, and gives rise to an uncertainty of 2–20%. For smaller differences between the $m_{\tilde{t}_2}$ and $m_{\tilde{t}_1}$ mass values, uncertainties in the modeling of initial-state radiation (ISR) become important. The uncertainty related to the PDFs on the acceptance is determined using the PDF4LHC recommendations [73] and contributes 2–5%. The corresponding uncertainty in the signal selection efficiency is of 3–15%, increasing for smaller $m_{\tilde{t}_2} - m_{\tilde{t}_1}$ mass differences. The systematic uncertainties, including their correlations, are treated consistently in the different analyses. The correlations between the different analyses have a small impact on the combined result.

Table 5: Relative systematic uncertainties (in percent) in the signal yields for the different event selections: one lepton (1ℓ), two OS leptons ($2 \text{ OS } \ell$), two SS leptons ($2 \text{ SS } \ell$), and at least three leptons ($\geq 3 \ell$). The range indicates the variation in the systematic uncertainty for the different decay channels and SRs considered.

Source	1ℓ [%]	$2 \text{ OS } \ell$ [%]	$2 \text{ SS } \ell$ [%]	$\geq 3 \ell$ [%]
Luminosity [74]		2.6		
Pileup modeling		< 5		
Trigger efficiency	3	6	6	5
Lepton identification and isolation efficiency	5	10	10	12
Jet energy scale modeling	1–3	1–3	1–10	5–15
b-jet identification [36]	3–5	3–5	2–10	5–20
ISR modeling [19]	3–5	3–5	3–15	3–15
PDFs	5	5	2	4
Total	9–11	14–15	14–23	15–30

Figure 5 (left) shows the 95% CL upper limits on the cross section times branching fraction

in the $m_{\tilde{t}_1}$ versus $m_{\tilde{t}_2}$ plane for the (a) $\tilde{t}_2 \rightarrow H\tilde{t}_1$ and (b) $\tilde{t}_2 \rightarrow Z\tilde{t}_1$ decay modes. The contour bounds the excluded region in the plane assuming the NLO+NLL cross section calculation in the decoupling limit for all the SUSY sparticles not included in the model. The results are presented assuming a branching fraction of 100% to each decay mode. The 95% CL expected (thick dashed) and observed (solid black) limits are obtained including all uncertainties with the exception of the theoretical uncertainty in the signal production cross section. The expected limit is defined as the median of the upper-limit distribution obtained using pseudo-experiments and the likelihood model considered. The bands around the expected limit correspond to the impact of experimental uncertainties, and the bands around the observed limit indicate the change for a ± 1 standard deviation (σ) variation in the theoretical cross section (mainly due to uncertainties in the renormalization/factorization scales and in the knowledge of the PDFs). In the $\tilde{t}_2 \rightarrow H\tilde{t}_1$ decay mode, taking a -1σ theory lower bound on signal cross sections, a \tilde{t}_2 squark with $m_{\tilde{t}_2} \lesssim 525$ GeV is excluded at a 95% CL for \tilde{t}_1 squarks with $m_{\tilde{t}_1} \lesssim 300$ GeV. Similarly, in the $\tilde{t}_2 \rightarrow Z\tilde{t}_1$ decay mode, a \tilde{t}_2 squark with $m_{\tilde{t}_2} \lesssim 575$ GeV is excluded at 95% CL for \tilde{t}_1 squark with $m_{\tilde{t}_1} \lesssim 400$ GeV.

For the pure $\tilde{t}_2 \rightarrow H\tilde{t}_1$ decay (Fig. 5 upper right), the SRs with at least three leptons, no $Z \rightarrow \ell^+ \ell^-$ candidates, and large b-jet multiplicities are the most sensitive. Nevertheless, the SRs with lower lepton multiplicities (one lepton or two leptons) have significant expected sensitivity in the $\tilde{t}_2 \rightarrow H\tilde{t}_1$ decay mode. Including the final states with lower lepton multiplicities in the combination lowers the cross section upper limit results by 15–20% compared to the three-lepton results alone. Therefore, all lepton multiplicity categories are used in the interpretation of the $t\bar{t}HH$ signal.

In the case of the signals with Z bosons (Fig. 5 lower right), the SRs with at least three leptons completely dominate the expected sensitivity. The different SRs with at least three leptons provide sensitivity to different types of signals. In particular, off-Z SRs are sensitive to the region of parameter space in which the Z bosons are off-shell, $m_{\tilde{t}_2} - m_{\tilde{t}_1} < m_Z$, while the on-Z regions provide sensitivity to signals with larger mass differences. Only the SRs with at least three leptons are used in the interpretation of the $t\bar{t}ZZ$ signal.

Mixed-decay scenarios, with non-zero branching fractions for the Z and H decay modes, are also considered, assuming these to be the only decay modes possible. Figure 6 shows the corresponding limits as a function of the relative branching fraction of the Z and H decay modes. The scenario with the least expected sensitivity is where the H boson decay mode dominates, while the best expected sensitivity is achieved when the Z boson decay mode dominates.

The cross section upper limits are obtained neglecting the contribution of direct \tilde{t}_1 squark pair production, which can satisfy the selection criteria for the single-lepton or OS-lepton SRs if a light-parton jet is misidentified as a b jet or if there is additional radiation leading to genuine b jets. Including direct \tilde{t}_1 squark pair production in the single-lepton or two OS lepton SRs typically lowers the cross section limit by a few percent, with the most pronounced differences occurring at larger \tilde{t}_2 mass. The contribution in the case of events with two SS leptons or at least three leptons is small due to the low probability of misidentifying non-prompt leptons. Since the signature with three leptons has the best sensitivity overall, the impact on the combined limit is much smaller than the uncertainty in the production cross section.

8 Summary

This letter presents results of a search for the pair production of the heavier top-squark mass eigenstate \tilde{t}_2 decaying to the lighter eigenstate \tilde{t}_1 , producing a signature of a top-antitop quark

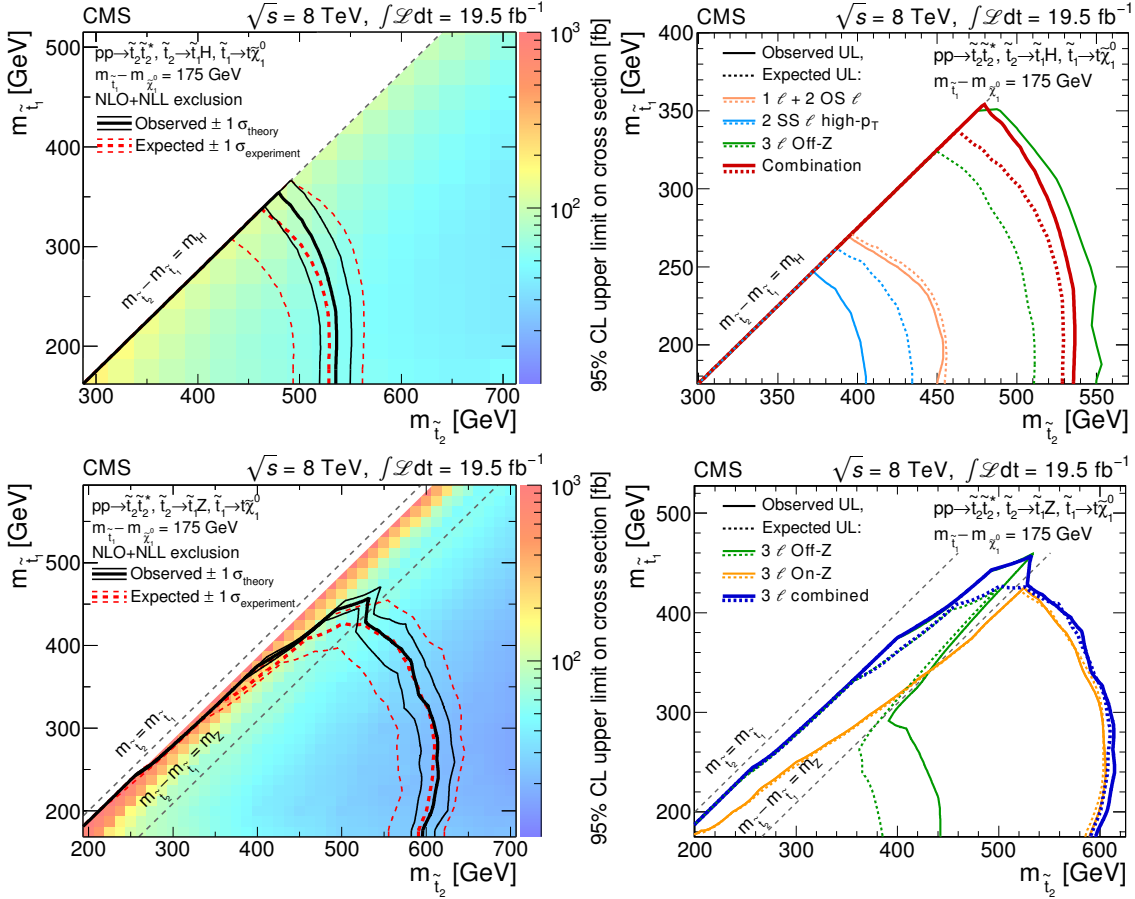


Figure 5: Interpretation of the results in SUSY simplified model parameter space, $m_{\tilde{t}_1}$ vs. $m_{\tilde{t}_2}$, with the neutralino mass constrained by the relation $m_{\tilde{t}_1} - m_{\tilde{\chi}_1^0} = 175$ GeV. The shaded maps (plots on the left) show the upper limit (95% CL) on the cross section times branching fraction at each point in the $m_{\tilde{t}_1}$ vs. $m_{\tilde{t}_2}$ plane for the process $pp \rightarrow \tilde{t}_2 \tilde{t}_2^*$, with $\tilde{t}_2 \rightarrow H \tilde{t}_1$, $\tilde{t}_1 \rightarrow \tilde{t}_1 \tilde{\chi}_1^0$ (upper plots) and $\tilde{t}_2 \rightarrow Z \tilde{t}_1$, $\tilde{t}_1 \rightarrow \tilde{t}_1 \tilde{\chi}_1^0$ (lower plots). In these plots, the results from all channels are combined. The excluded region in the $m_{\tilde{t}_1}$ vs. $m_{\tilde{t}_2}$ parameter space is obtained by comparing the cross section times branching fraction upper limit at each model point with the corresponding NLO+NLL cross section for the process, assuming that (a) $\mathcal{B}(\tilde{t}_2 \rightarrow H \tilde{t}_1) = 100\%$ or (b) that $\mathcal{B}(\tilde{t}_2 \rightarrow Z \tilde{t}_1) = 100\%$. The solid (dashed) curves define the boundary of the observed (expected) excluded region. The ± 1 standard deviation (σ) bands are indicated by the finer contours. The figures on the right show the observed (expected) exclusion contours, which are indicated by the solid (dashed) curves for the contributing channels. As indicated in the legends of the right-hand figures, the thinner curves show the results from each of the contributing channels, while the thicker curve shows their combination. The four event categories for the $\tilde{t}_2 \rightarrow H \tilde{t}_1$ study are shown in the upper plots, while the on-Z and off-Z categories for events with at least three leptons are shown in the lower plots.

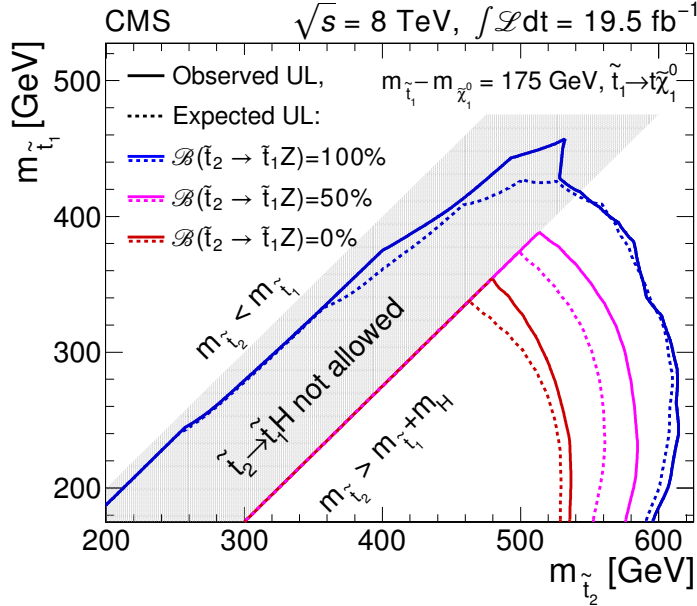


Figure 6: Upper limits on the cross section for \tilde{t}_2 pair production for different branching fractions of $\tilde{t}_2 \rightarrow H\tilde{t}_1$ and $\tilde{t}_2 \rightarrow Z\tilde{t}_1$, assuming that $\mathcal{B}(\tilde{t}_2 \rightarrow H\tilde{t}_1) + \mathcal{B}(\tilde{t}_2 \rightarrow Z\tilde{t}_1) = 100\%$. The \tilde{t}_1 squark is assumed to always decay to a top quark and a neutralino $\tilde{\chi}_1^0$ with $m_{\tilde{t}_1} - m_{\tilde{\chi}_1^0} = m_t$. The decay $\tilde{t}_2 \rightarrow H\tilde{t}_1$ is only considered when the H boson production is kinematically allowed, $m_{\tilde{t}_2} - m_{\tilde{t}_1} > m_H$.

pair in association with Higgs or Z bosons. The analysis explores final states with exactly one lepton and at least three identified bottom-quark jets (b jets), with exactly two leptons of opposite charge and at least three b jets, with exactly two same-sign leptons and at least one b jet, and with three or more leptons and at least one b jet, where by “lepton” we mean an electron or muon. No significant excess event yield above standard model expectations is observed. The results are used to exclude a range of \tilde{t}_2 masses below approximately 575 GeV for \tilde{t}_1 masses below approximately 400 GeV. The interpretation assumes that the \tilde{t}_1 squark always decays to $\tilde{\chi}_1^0$ and that $m_{\tilde{t}_1} - m_{\tilde{\chi}_1^0} \simeq m_t$, where the $\tilde{\chi}_1^0$ particle represents a stable, weakly interacting lightest supersymmetric particle neutralino whose signature in the detector is missing transverse energy. This region of phase space is not probed by searches for direct \tilde{t}_1 squark pair production.

Acknowledgements

We congratulate our colleagues in the CERN accelerator departments for the excellent performance of the LHC and thank the technical and administrative staffs at CERN and at other CMS institutes for their contributions to the success of the CMS effort. In addition, we gratefully acknowledge the computing centers and personnel of the Worldwide LHC Computing Grid for delivering so effectively the computing infrastructure essential to our analyses. Finally, we acknowledge the enduring support for the construction and operation of the LHC and the CMS detector provided by the following funding agencies: BMWFW and FWF (Austria); FNRS and FWO (Belgium); CNPq, CAPES, FAPERJ, and FAPESP (Brazil); MES (Bulgaria); CERN; CAS, MoST, and NSFC (China); COLCIENCIAS (Colombia); MSES and CSF (Croatia); RPF (Cyprus); MoER, ERC IUT and ERDF (Estonia); Academy of Finland, MEC, and HIP (Finland); CEA and CNRS/IN2P3 (France); BMBF, DFG, and HGF (Germany); GSRT (Greece); OTKA and NIH

(Hungary); DAE and DST (India); IPM (Iran); SFI (Ireland); INFN (Italy); NRF and WCU (Republic of Korea); LAS (Lithuania); MOE and UM (Malaysia); CINVESTAV, CONACYT, SEP, and UASLP-FAI (Mexico); MBIE (New Zealand); PAEC (Pakistan); MSHE and NSC (Poland); FCT (Portugal); JINR (Dubna); MON, RosAtom, RAS and RFBR (Russia); MESTD (Serbia); SEIDI and CPAN (Spain); Swiss Funding Agencies (Switzerland); MST (Taipei); ThEPCenter, IPST, STAR and NSTDA (Thailand); TUBITAK and TAEK (Turkey); NASU and SFFR (Ukraine); STFC (United Kingdom); DOE and NSF (USA).

Individuals have received support from the Marie-Curie programme and the European Research Council and EPLANET (European Union); the Leventis Foundation; the Alfred P. Sloan Foundation; the Alexander von Humboldt Foundation; the Belgian Federal Science Policy Office; the Fonds pour la Formation à la Recherche dans l'Industrie et dans l'Agriculture (FRIA-Belgium); the Agentschap voor Innovatie door Wetenschap en Technologie (IWT-Belgium); the Ministry of Education, Youth and Sports (MEYS) of the Czech Republic; the Council of Science and Industrial Research, India; the Compagnia di San Paolo (Torino); the HOMING PLUS programme of Foundation For Polish Science, cofinanced by EU, Regional Development Fund; and the Thalis and Aristeia programmes cofinanced by EU-ESF and the Greek NSRF.

References

- [1] G. R. Farrar and P. Fayet, “Phenomenology of the production, decay, and detection of new hadronic states associated with supersymmetry”, *Phys. Lett. B* **76** (1978) 575, doi:10.1016/0370-2693(78)90858-4.
- [2] S. Dimopoulos and S. Raby, “Supercolor”, *Nucl. Phys. B* **192** (1981) 353, doi:10.1016/0550-3213(81)90430-2.
- [3] E. Witten, “Dynamical breaking of supersymmetry”, *Nucl. Phys. B* **188** (1981) 513, doi:10.1016/0550-3213(81)90006-7.
- [4] M. Dine, W. Fischler, and M. Srednicki, “Supersymmetric technicolor”, *Nucl. Phys. B* **189** (1981) 575, doi:10.1016/0550-3213(81)90582-4.
- [5] S. Dimopoulos and H. Georgi, “Softly broken supersymmetry and SU(5)”, *Nucl. Phys. B* **193** (1981) 150, doi:10.1016/0550-3213(81)90522-8.
- [6] N. Sakai, “Naturalness in supersymmetric GUTS”, *Z. Phys. C* **11** (1981) 153, doi:10.1007/BF01573998.
- [7] R. K. Kaul and P. Majumdar, “Cancellation of quadratically divergent mass corrections in globally supersymmetric spontaneously broken gauge theories”, *Nucl. Phys. B* **199** (1982) 36, doi:10.1016/0550-3213(82)90565-X.
- [8] R. Barbieri and G. F. Giudice, “Upper bounds on supersymmetric particle masses”, *Nucl. Phys. B* **306** (1988) 63, doi:10.1016/0550-3213(88)90171-X.
- [9] B. de Carlos and J. A. Casas, “One-loop analysis of the electroweak breaking in supersymmetric models and the fine-tuning problem”, *Phys. Lett. B* **309** (1993) 320, doi:10.1016/0370-2693(93)90940-J, arXiv:hep-ph/9303291.
- [10] S. Dimopoulos and G. F. Giudice, “Naturalness constraints in supersymmetric theories with non-universal soft terms”, *Phys. Lett. B* **357** (1995) 573, doi:10.1016/0370-2693(95)00961-J, arXiv:hep-ph/9507282.

- [11] R. Barbieri, G. Dvali, and L. J. Hall, “Predictions from a U(2) flavour symmetry in supersymmetric theories”, *Phys. Lett. B* **377** (1996) 76,
doi:10.1016/0370-2693(96)00318-8, arXiv:hep-ph/9512388.
- [12] M. Papucci, J. T. Ruderman, and A. Weiler, “Natural SUSY endures”, *JHEP* **09** (2012) 035,
doi:10.1007/JHEP09(2012)035, arXiv:1110.6926.
- [13] ATLAS Collaboration, “Search for a supersymmetric partner to the top quark in final states with jets and missing transverse momentum at $\sqrt{s} = 7$ TeV with the ATLAS detector”, *Phys. Rev. Lett.* **109** (2012) 211802,
doi:10.1103/PhysRevLett.109.211802, arXiv:1208.1447.
- [14] ATLAS Collaboration, “Search for direct top squark pair production in final states with one isolated lepton, jets, and missing transverse momentum in $\sqrt{s} = 7$ TeV pp collisions using 4.7 fb^{-1} of ATLAS data”, *Phys. Rev. Lett.* **109** (2012) 211803,
doi:10.1103/PhysRevLett.109.211803, arXiv:1208.2590.
- [15] ATLAS Collaboration, “Search for light scalar top quark pair production in final states with two leptons with the ATLAS detector in $\sqrt{s} = 7$ TeV proton-proton collisions”, *Eur. Phys. J. C* **72** (2012) 2237, doi:10.1140/epjc/s10052-012-2237-1,
arXiv:1208.4305.
- [16] ATLAS Collaboration, “Search for light top squark pair production in final states with leptons and b-jets with the ATLAS detector in $\sqrt{s} = 7$ TeV proton-proton collisions”, *Phys. Lett. B* **720** (2013) 13, doi:10.1016/j.physletb.2013.01.049,
arXiv:1209.2102.
- [17] ATLAS Collaboration, “Search for direct third-generation squark pair production in final states with missing transverse momentum and two b-jets in $\sqrt{s} = 8$ TeV pp collisions with the ATLAS detector”, *JHEP* **10** (2013) 189, doi:10.1007/JHEP10(2013)189,
arXiv:1308.2631.
- [18] ATLAS Collaboration, “Search for direct top-squark pair production in final states with two leptons in pp collisions at $\sqrt{s} = 8$ TeV with the ATLAS detector”, *JHEP* **06** (2014) 124, doi:10.1007/JHEP06(2014)124, arXiv:1403.4853.
- [19] CMS Collaboration, “Search for top-squark pair production in the single-lepton final state in pp collisions at $\sqrt{s} = 8$ TeV”, *Eur. Phys. J. C* **73** (2013) 2677,
doi:10.1140/epjc/s10052-013-2677-2, arXiv:1308.1586.
- [20] T. Han, R. Mahbubani, D. G. E. Walker, and L.-T. Wang, “Top-quark pair plus large missing energy at the LHC”, *JHEP* **05** (2009) 117,
doi:10.1088/1126-6708/2009/05/117, arXiv:0803.3820.
- [21] CMS Collaboration, “Search for supersymmetry in pp collisions at $\sqrt{s}=8$ TeV in events with a single lepton, large jet multiplicity, and multiple b jets”, *Phys. Lett. B* **733** (2014) 328, doi:10.1016/j.physletb.2014.04.023, arXiv:1311.4937.
- [22] CMS Collaboration, “Search for gluino mediated bottom- and top-squark production in multijet final states in pp collisions at 8 TeV”, *Phys. Lett. B* **725** (2013) 243,
doi:10.1016/j.physletb.2013.06.058, arXiv:1305.2390.

- [23] ATLAS Collaboration, “Search for scalar top quark pair production in natural gauge mediated supersymmetry models with the ATLAS detector in pp collisions at $\sqrt{s} = 7 \text{ TeV}$ ”, *Phys. Lett. B* **715** (2012) 44, doi:10.1016/j.physletb.2012.07.010, arXiv:1204.6736.
- [24] ATLAS Collaboration, “Search for direct top squark pair production in events with a Z boson, b-jets and missing transverse momentum in $\sqrt{s} = 8 \text{ TeV}$ pp collisions with the ATLAS detector”, *Eur. Phys. J. C* **74** (2014) 2883, doi:10.1140/epjc/s10052-014-2883-6, arXiv:1403.5222.
- [25] CMS Collaboration, “The CMS experiment at the CERN LHC”, *J. Instrum.* **3** (2008) S08004, doi:10.1088/1748-0221/3/08/S08004.
- [26] CMS Collaboration, “Particle-Flow Event Reconstruction in CMS and Performance for Jets, Taus, and MET”, CMS Physics Analysis Summary CMS-PAS-PFT-09-001, 2009.
- [27] CMS Collaboration, “Commissioning of the Particle-flow Event Reconstruction with the first LHC collisions recorded in the CMS detector”, CMS Physics Analysis Summary CMS-PAS-PFT-10-001, 2010.
- [28] CMS Collaboration, “Electron reconstruction and identification at $\sqrt{s} = 7 \text{ TeV}$ ”, CMS Physics Analysis Summary CMS-PAS-EGM-10-004, 2010.
- [29] CMS Collaboration, “Energy calibration and resolution of the CMS electromagnetic calorimeter in pp collisions at $\sqrt{s} = 7 \text{ TeV}$ ”, *J. Instrum.* **8** (2013) P09009, doi:10.1088/1748-0221/8/09/P09009, arXiv:1306.2016.
- [30] CMS Collaboration, “Performance of CMS muon reconstruction in pp collision events at $\sqrt{s} = 7 \text{ TeV}$ ”, *J. Instrum.* **7** (2012) P10002, doi:10.1088/1748-0221/7/10/P10002, arXiv:1206.4071.
- [31] CMS Collaboration, “Search for new physics in events with same-sign dileptons and jets in pp collisions at 8 TeV”, *JHEP* **01** (2014) 163, doi:10.1007/JHEP01(2014)163, arXiv:1311.6736.
- [32] CMS Collaboration, “Evidence for the 125 GeV Higgs boson decaying to a pair of τ leptons”, *JHEP* **05** (2014) 104, doi:10.1007/JHEP05(2014)104, arXiv:1401.5041.
- [33] M. Cacciari, G. P. Salam, and G. Soyez, “The anti- k_t jet clustering algorithm”, *JHEP* **04** (2008) 063, doi:10.1088/1126-6708/2008/04/063, arXiv:0802.1189.
- [34] CMS Collaboration, “Determination of jet energy calibration and transverse momentum resolution in CMS”, *J. Instrum.* **6** (2011) P11002, doi:10.1088/1748-0221/6/11/P11002, arXiv:1107.4277.
- [35] M. Cacciari and G. P. Salam, “Pileup subtraction using jet areas”, *Phys. Lett. B* **659** (2008) 119, doi:10.1016/j.physletb.2007.09.077, arXiv:0707.1378.
- [36] CMS Collaboration, “Identification of b-quark jets with the CMS experiment”, *J. Instrum.* **8** (2013) P04013, doi:10.1088/1748-0221/8/04/P04013, arXiv:1211.4462.
- [37] CMS Collaboration, “MET performance in 8 TeV data”, CMS Physics Analysis Summary CMS-PAS-JME-12-002, 2013.

- [38] J. Alwall et al., “MadGraph 5: going beyond”, *JHEP* **06** (2011) 128, doi:10.1007/JHEP06(2011)128, arXiv:1106.0522.
- [39] T. Sjöstrand, S. Mrenna, and P. Skands, “PYTHIA 6.4 physics and manual”, *JHEP* **05** (2006) 026, doi:10.1088/1126-6708/2006/05/026, arXiv:hep-ph/0603175.
- [40] CMS Collaboration, “Interpretation of searches for supersymmetry with simplified models”, *Phys. Rev. D* **88** (2013) 052017, doi:10.1103/PhysRevD.88.052017, arXiv:1301.2175.
- [41] CMS Collaboration, “Observation of a new boson at a mass of 125 GeV with the CMS experiment at the LHC”, *Phys. Lett. B* **716** (2012) 30, doi:10.1016/j.physletb.2012.08.021, arXiv:1207.7235.
- [42] S. Dittmaier et al., “Handbook of LHC Higgs Cross Sections: 2. Differential Distributions”, (2012). arXiv:1201.3084.
- [43] W. Beenakker, R. Höpker, M. Spira, and P. M. Zerwas, “Squark and gluino production at hadron colliders”, *Nucl. Phys. B* **492** (1997) 51, doi:10.1016/S0550-3213(97)80027-2, arXiv:hep-ph/9610490.
- [44] A. Kulesza and L. Motyka, “Threshold resummation for squark-antisquark and gluino-pair production at the LHC”, *Phys. Rev. Lett.* **102** (2009) 111802, doi:10.1103/PhysRevLett.102.111802, arXiv:0807.2405.
- [45] A. Kulesza and L. Motyka, “Soft gluon resummation for the production of gluino-gluino and squark-antisquark pairs at the LHC”, *Phys. Rev. D* **80** (2009) 095004, doi:10.1103/PhysRevD.80.095004, arXiv:0905.4749.
- [46] W. Beenakker et al., “Soft-gluon resummation for squark and gluino hadroproduction”, *JHEP* **12** (2009) 041, doi:10.1088/1126-6708/2009/12/041, arXiv:0909.4418.
- [47] W. Beenakker et al., “Squark and gluino hadroproduction”, *Int. J. Mod. Phys. A* **26** (2011) 2637, doi:10.1142/S0217751X11053560, arXiv:1105.1110.
- [48] M. Krämer et al., “Supersymmetry production cross sections in pp collisions at $\sqrt{s} = 7$ TeV”, (2012). arXiv:1206.2892.
- [49] S. Alioli, P. Nason, C. Oleari, and E. Re, “NLO single-top production matched with shower in POWHEG: s- and t-channel contributions”, *JHEP* **09** (2009) 111, doi:10.1088/1126-6708/2009/09/111, arXiv:0907.4076. [Erratum: doi:10.1007/JHEP02(2010)011].
- [50] E. Re, “Single-top Wt-channel production matched with parton showers using the POWHEG method”, *Eur. Phys. J. C* **71** (2011) 1547, doi:10.1140/epjc/s10052-011-1547-z, arXiv:1009.2450.
- [51] S. Frixione and B. R. Webber, “Matching NLO QCD computations and parton shower simulations”, *JHEP* **06** (2002) 029, doi:10.1088/1126-6708/2002/06/029, arXiv:hep-ph/0204244.
- [52] S. Frixione, P. Nason, and B. R. Webber, “Matching NLO QCD and parton showers in heavy flavor production”, *JHEP* **08** (2003) 007, doi:10.1088/1126-6708/2003/08/007, arXiv:hep-ph/0305252.

- [53] H.-L. Lai et al., “New parton distributions for collider physics”, *Phys. Rev. D* **82** (2010) 074024, doi:10.1103/PhysRevD.82.074024, arXiv:1007.2241.
- [54] Pumplin et al., “New generation of parton distributions with uncertainties from global QCD analysis”, *JHEP* **07** (2002) 012, doi:10.1088/1126-6708/2002/07/012, arXiv:hep-ph/0201195.
- [55] N. Kidonakis, “Differential and total cross sections for top pair and single top production”, (2012). arXiv:1205.3453.
- [56] J. M. Campbell and R. K. Ellis, “ $t\bar{t}W^\pm$ production and decay at NLO”, *JHEP* **07** (2012) 052, doi:10.1007/JHEP07(2012)052, arXiv:1204.5678.
- [57] M. V. Garzelli, A. Kardos, C. G. Papadopoulos, and Z. Trocsanyi, “ $t\bar{t}W^\pm$ and $t\bar{t}Z$ hadroproduction at NLO accuracy in QCD with parton shower and hadronization effects”, *JHEP* **11** (2012) 056, doi:10.1007/JHEP11(2012)056, arXiv:1208.2665.
- [58] J. M. Campbell and R. K. Ellis, “MCFM for the Tevatron and the LHC”, *Nucl. Phys. Proc. Suppl.* **205** (2010) 10, doi:10.1016/j.nuclphysbps.2010.08.011, arXiv:1007.3492.
- [59] R. Gavin, Y. Li, F. Petriello, and S. Quackenbush, “W Physics at the LHC with FEWZ 2.1”, *Comput. Phys. Commun.* **184** (2013) 208, doi:10.1016/j.cpc.2012.09.005, arXiv:1201.5896.
- [60] R. Frederix et al., “Four-lepton production at hadron colliders: aMC@NLO predictions with theoretical uncertainties”, *JHEP* **02** (2012) 099, doi:10.1007/JHEP02(2012)099, arXiv:1110.4738.
- [61] GEANT4 Collaboration, “GEANT4—a simulation toolkit”, *Nucl. Instrum. Meth. A* **506** (2003) 250, doi:10.1016/S0168-9002(03)01368-8.
- [62] S. Abdullin et al., “The fast Simulation of the CMS Detector at LHC”, in *Int. Conf. on Computing in High Energy Physics (CHEP 2010)*, p. 032049. 2011. *J. Phys.: Conf. Ser.* 331. doi:10.1088/1742-6596/331/3/032049.
- [63] R. Rahmat, R. Kroeger, and A. Giannanco, “The fast simulation of the CMS experiment”, in *Int. Conf. on Computing in High Energy Physics (CHEP 2012)*, p. 062016. 2012. *J. Phys.: Conf. Ser.* 396. doi:10.1088/1742-6596/396/6/062016.
- [64] CMS Collaboration, “CMS strategies for tau reconstruction and identification using particle-flow techniques”, CMS Physics Analysis Summary CMS-PAS-PFT-08-001, 2009.
- [65] CMS Collaboration, “Study of tau reconstruction algorithms using pp collisions data collected at $\sqrt{s} = 7$ TeV”, CMS Physics Analysis Summary CMS-PAS-PFT-10-004, 2010.
- [66] CMS Collaboration, “Performance of τ lepton reconstruction and identification in CMS”, *J. Instrum.* **7** (2012) P01001, doi:10.1088/1748-0221/7/01/P01001, arXiv:1109.6034.
- [67] CMS Collaboration, “Pileup Jet Identification”, CMS Physics Analysis Summary CMS-PAS-JME-13-005, 2013.

- [68] CMS Collaboration, “Measurement of associated production of vector bosons and top quark-antiquark pairs at $\sqrt{s} = 7 \text{ TeV}$ ”, *Phys. Rev. Lett.* **110** (2013) 172002, doi:10.1103/PhysRevLett.110.172002, arXiv:1303.3239.
- [69] R. D. Cousins, J. T. Linnemann, and J. Tucker, “Evaluation of three methods for calculating statistical significance when incorporating a systematic uncertainty into a test of the background-only hypothesis for a Poisson process”, *Nucl. Instrum. Meth. A* **595** (2008) 480, doi:10.1016/j.nima.2008.07.086, arXiv:physics/0702156.
- [70] T. Junk, “Confidence level computation for combining searches with small statistics”, *Nucl. Instrum. Meth. A* **434** (1999) 435, doi:10.1016/S0168-9002(99)00498-2, arXiv:hep-ex/9902006.
- [71] A. L. Read, “Presentation of search results: the CL_S technique”, *J. Phys. G* **28** (2002) 2693, doi:10.1088/0954-3899/28/10/313.
- [72] ATLAS and CMS Collaborations, LHC Higgs Combination Group, “Procedure for the LHC Higgs boson search combination in Summer 2011”, Technical Report ATL-PHYS-PUB 2011-11, CMS NOTE 2011/005, 2011.
- [73] M. Botje et al., “The PDF4LHC Working Group Interim Recommendations”, (2011). arXiv:1101.0538.
- [74] CMS Collaboration, “CMS luminosity based on pixel cluster counting — Summer 2013 update”, CMS Physics Analysis Summary CMS-PAS-LUM-13-001, 2013.

A The CMS Collaboration

Yerevan Physics Institute, Yerevan, Armenia
V. Khachatryan, A.M. Sirunyan, A. Tumasyan

Institut für Hochenergiephysik der OeAW, Wien, Austria

W. Adam, T. Bergauer, M. Dragicevic, J. Erö, C. Fabjan¹, M. Friedl, R. Frühwirth¹, V.M. Ghete,
C. Hartl, N. Hörmann, J. Hrubec, M. Jeitler¹, W. Kiesenhofer, V. Knünz, M. Krammer¹,
I. Krätschmer, D. Liko, I. Mikulec, D. Rabady², B. Rahbaran, H. Rohringer, R. Schöfbeck,
J. Strauss, A. Taurok, W. Treberer-Treberspurg, W. Waltenberger, C.-E. Wulz¹

National Centre for Particle and High Energy Physics, Minsk, Belarus

V. Mossolov, N. Shumeiko, J. Suarez Gonzalez

Universiteit Antwerpen, Antwerpen, Belgium

S. Alderweireldt, M. Bansal, S. Bansal, T. Cornelis, E.A. De Wolf, X. Janssen, A. Knutsson,
S. Luyckx, S. Ochesanu, B. Roland, R. Rougny, M. Van De Klundert, H. Van Haevermaet, P. Van
Mechelen, N. Van Remortel, A. Van Spilbeeck

Vrije Universiteit Brussel, Brussel, Belgium

F. Blekman, S. Blyweert, J. D'Hondt, N. Daci, N. Heracleous, A. Kalogeropoulos, J. Keaveney,
T.J. Kim, S. Lowette, M. Maes, A. Olbrechts, Q. Python, D. Strom, S. Tavernier, W. Van Doninck,
P. Van Mulders, G.P. Van Onsem, I. Villella

Université Libre de Bruxelles, Bruxelles, Belgium

C. Caillol, B. Clerbaux, G. De Lentdecker, D. Dobur, L. Favart, A.P.R. Gay, A. Grebenyuk,
A. Léonard, A. Mohammadi, L. Perniè², T. Reis, T. Seva, L. Thomas, C. Vander Velde, P. Vanlaer,
J. Wang

Ghent University, Ghent, Belgium

V. Adler, K. Beernaert, L. Benucci, A. Cimmino, S. Costantini, S. Crucy, S. Dildick, A. Fagot,
G. Garcia, B. Klein, J. Mccartin, A.A. Ocampo Rios, D. Ryckbosch, S. Salva Diblen, M. Sigamani,
N. Strobbe, F. Thyssen, M. Tytgat, E. Yazgan, N. Zaganidis

Université Catholique de Louvain, Louvain-la-Neuve, Belgium

S. Basegmez, C. Beluffi³, G. Bruno, R. Castello, A. Caudron, L. Ceard, G.G. Da Silveira,
C. Delaere, T. du Pree, D. Favart, L. Forthomme, A. Giannanco⁴, J. Hollar, P. Jez, M. Komm,
V. Lemaitre, J. Liao, C. Nuttens, D. Pagano, L. Perrini, A. Pin, K. Piotrkowski, A. Popov⁵,
L. Quertenmont, M. Selvaggi, M. Vidal Marono, J.M. Vizan Garcia

Université de Mons, Mons, Belgium

N. Belyi, T. Caebergs, E. Daubie, G.H. Hammad

Centro Brasileiro de Pesquisas Fisicas, Rio de Janeiro, Brazil

W.L. Aldá Júnior, G.A. Alves, M. Correa Martins Junior, T. Dos Reis Martins, M.E. Pol

Universidade do Estado do Rio de Janeiro, Rio de Janeiro, Brazil

W. Carvalho, J. Chinellato⁶, A. Custódio, E.M. Da Costa, D. De Jesus Damiao, C. De Oliveira
Martins, S. Fonseca De Souza, H. Malbouisson, M. Malek, D. Matos Figueiredo, L. Mundim,
H. Nogima, W.L. Prado Da Silva, J. Santaolalla, A. Santoro, A. Sznajder, E.J. Tonelli Manganote⁶,
A. Vilela Pereira

Universidade Estadual Paulista ^a, Universidade Federal do ABC ^b, São Paulo, Brazil

C.A. Bernardes^b, F.A. Dias^{a,7}, T.R. Fernandez Perez Tomei^a, E.M. Gregores^b, P.G. Mercadante^b,
S.F. Novaes^a, Sandra S. Padula^a

Institute for Nuclear Research and Nuclear Energy, Sofia, Bulgaria

A. Aleksandrov, V. Genchev², P. Iaydjiev, A. Marinov, S. Piperov, M. Rodozov, G. Sultanov, M. Vutova

University of Sofia, Sofia, Bulgaria

A. Dimitrov, I. Glushkov, R. Hadjiiska, V. Kozhuharov, L. Litov, B. Pavlov, P. Petkov

Institute of High Energy Physics, Beijing, China

J.G. Bian, G.M. Chen, H.S. Chen, M. Chen, R. Du, C.H. Jiang, D. Liang, S. Liang, R. Plestina⁸, J. Tao, X. Wang, Z. Wang

State Key Laboratory of Nuclear Physics and Technology, Peking University, Beijing, China

C. Asawatangtrakuldee, Y. Ban, Y. Guo, Q. Li, W. Li, S. Liu, Y. Mao, S.J. Qian, D. Wang, L. Zhang, W. Zou

Universidad de Los Andes, Bogota, Colombia

C. Avila, L.F. Chaparro Sierra, C. Florez, J.P. Gomez, B. Gomez Moreno, J.C. Sanabria

Technical University of Split, Split, Croatia

N. Godinovic, D. Lelas, D. Polic, I. Puljak

University of Split, Split, Croatia

Z. Antunovic, M. Kovac

Institute Rudjer Boskovic, Zagreb, Croatia

V. Brigljevic, K. Kadija, J. Luetic, D. Mekterovic, L. Sudic

University of Cyprus, Nicosia, Cyprus

A. Attikis, G. Mavromanolakis, J. Mousa, C. Nicolaou, F. Ptochos, P.A. Razis

Charles University, Prague, Czech Republic

M. Bodlak, M. Finger, M. Finger Jr.

Academy of Scientific Research and Technology of the Arab Republic of Egypt, Egyptian Network of High Energy Physics, Cairo, Egypt

Y. Assran⁹, A. Ellithi Kamel¹⁰, M.A. Mahmoud¹¹, A. Radi^{12,13}

National Institute of Chemical Physics and Biophysics, Tallinn, Estonia

M. Kadastik, M. Murumaa, M. Raidal, A. Tiko

Department of Physics, University of Helsinki, Helsinki, Finland

P. Eerola, G. Fedi, M. Voutilainen

Helsinki Institute of Physics, Helsinki, Finland

J. Hätkönen, V. Karimäki, R. Kinnunen, M.J. Kortelainen, T. Lampén, K. Lassila-Perini, S. Lehti, T. Lindén, P. Luukka, T. Mäenpää, T. Peltola, E. Tuominen, J. Tuominiemi, E. Tuovinen, L. Wendland

Lappeenranta University of Technology, Lappeenranta, Finland

T. Tuuva

DSM/IRFU, CEA/Saclay, Gif-sur-Yvette, France

M. Besancon, F. Couderc, M. Dejardin, D. Denegri, B. Fabbro, J.L. Faure, C. Favaro, F. Ferri, S. Ganjour, A. Givernaud, P. Gras, G. Hamel de Monchenault, P. Jarry, E. Locci, J. Malcles, A. Nayak, J. Rander, A. Rosowsky, M. Titov

Laboratoire Leprince-Ringuet, Ecole Polytechnique, IN2P3-CNRS, Palaiseau, France

S. Baffioni, F. Beaudente, P. Busson, C. Charlot, T. Dahms, M. Dalchenko, L. Dobrzynski, N. Filipovic, A. Florent, R. Granier de Cassagnac, L. Mastrolorenzo, P. Miné, C. Mironov, I.N. Naranjo, M. Nguyen, C. Ochando, P. Paganini, R. Salerno, J.B. Sauvan, Y. Sirois, C. Veelken, Y. Yilmaz, A. Zabi

Institut Pluridisciplinaire Hubert Curien, Université de Strasbourg, Université de Haute Alsace Mulhouse, CNRS/IN2P3, Strasbourg, France

J.-L. Agram¹⁴, J. Andrea, A. Aubin, D. Bloch, J.-M. Brom, E.C. Chabert, C. Collard, E. Conte¹⁴, J.-C. Fontaine¹⁴, D. Gelé, U. Goerlach, C. Goetzmann, A.-C. Le Bihan, P. Van Hove

Centre de Calcul de l’Institut National de Physique Nucléaire et de Physique des Particules, CNRS/IN2P3, Villeurbanne, France

S. Gadrat

Université de Lyon, Université Claude Bernard Lyon 1, CNRS-IN2P3, Institut de Physique Nucléaire de Lyon, Villeurbanne, France

S. Beauceron, N. Beaupere, G. Boudoul², S. Brochet, C.A. Carrillo Montoya, J. Chasserat, R. Chierici, D. Contardo², P. Depasse, H. El Mamouni, J. Fan, J. Fay, S. Gascon, M. Gouzevitch, B. Ille, T. Kurca, M. Lethuillier, L. Mirabito, S. Perries, J.D. Ruiz Alvarez, D. Sabes, L. Sgandurra, V. Sordini, M. Vander Donckt, P. Verdier, S. Viret, H. Xiao

Institute of High Energy Physics and Informatization, Tbilisi State University, Tbilisi, Georgia

Z. Tsamalaidze¹⁵

RWTH Aachen University, I. Physikalisches Institut, Aachen, Germany

C. Autermann, S. Beranek, M. Bontenackels, B. Calpas, M. Edelhoff, L. Feld, O. Hindrichs, K. Klein, A. Ostapchuk, A. Perieanu, F. Raupach, J. Sammet, S. Schael, D. Sprenger, H. Weber, B. Wittmer, V. Zhukov⁵

RWTH Aachen University, III. Physikalisches Institut A, Aachen, Germany

M. Ata, J. Caudron, E. Dietz-Laursonn, D. Duchardt, M. Erdmann, R. Fischer, A. Güth, T. Hebbeker, C. Heidemann, K. Hoepfner, D. Klingebiel, S. Knutzen, P. Kreuzer, M. Merschmeyer, A. Meyer, M. Olschewski, K. Padeken, P. Papacz, H. Reithler, S.A. Schmitz, L. Sonnenschein, D. Teyssier, S. Thüer, M. Weber

RWTH Aachen University, III. Physikalisches Institut B, Aachen, Germany

V. Cherepanov, Y. Erdogan, G. Flügge, H. Geenen, M. Geisler, W. Haj Ahmad, F. Hoehle, B. Kargoll, T. Kress, Y. Kuessel, J. Lingemann², A. Nowack, I.M. Nugent, L. Perchalla, O. Pooth, A. Stahl

Deutsches Elektronen-Synchrotron, Hamburg, Germany

I. Asin, N. Bartosik, J. Behr, W. Behrenhoff, U. Behrens, A.J. Bell, M. Bergholz¹⁶, A. Bethani, K. Borras, A. Burgmeier, A. Cakir, L. Calligaris, A. Campbell, S. Choudhury, F. Costanza, C. Diez Pardos, S. Dooling, T. Dorland, G. Eckerlin, D. Eckstein, T. Eichhorn, G. Flucke, J. Garay Garcia, A. Geiser, P. Gunnellini, J. Hauk, G. Hellwig, M. Hempel, D. Horton, H. Jung, M. Kasemann, P. Katsas, J. Kieseler, C. Kleinwort, D. Krücker, W. Lange, J. Leonard, K. Lipka, A. Lobanov, W. Lohmann¹⁶, B. Lutz, R. Mankel, I. Marfin, I.-A. Melzer-Pellmann, A.B. Meyer, J. Mnich, A. Mussgiller, S. Naumann-Emme, O. Novgorodova, F. Nowak, E. Ntomari, H. Perrey, D. Pitzl, R. Placakyte, A. Raspereza, P.M. Ribeiro Cipriano, E. Ron, M.Ö. Sahin, J. Salfeld-Nebgen, P. Saxena, R. Schmidt¹⁶, T. Schoerner-Sadenius, M. Schröder, S. Spannagel, A.D.R. Vargas Trevino, R. Walsh, C. Wissing

University of Hamburg, Hamburg, Germany

M. Aldaya Martin, V. Blobel, M. Centis Vignali, J. Erfle, E. Garutti, K. Goebel, M. Görner, M. Gosselink, J. Haller, R.S. Höing, H. Kirschenmann, R. Klanner, R. Kogler, J. Lange, T. Lapsien, T. Lenz, I. Marchesini, J. Ott, T. Peiffer, N. Pietsch, D. Rathjens, C. Sander, H. Schettler, P. Schleper, E. Schlieckau, A. Schmidt, M. Seidel, J. Sibille¹⁷, V. Sola, H. Stadie, G. Steinbrück, D. Troendle, E. Usai, L. Vanelderen

Institut für Experimentelle Kernphysik, Karlsruhe, Germany

C. Barth, C. Baus, J. Berger, C. Böser, E. Butz, T. Chwalek, W. De Boer, A. Descroix, A. Dierlamm, M. Feindt, F. Frensch, F. Hartmann², T. Hauth², U. Husemann, I. Katkov⁵, A. Kornmayer², E. Kuznetsova, P. Lobelle Pardo, M.U. Mozer, Th. Müller, A. Nürnberg, G. Quast, K. Rabbertz, F. Ratnikov, S. Röcker, H.J. Simonis, F.M. Stober, R. Ulrich, J. Wagner-Kuhr, S. Wayand, T. Weiler, R. Wolf

Institute of Nuclear and Particle Physics (INPP), NCSR Demokritos, Aghia Paraskevi, Greece

G. Anagnostou, G. Daskalakis, T. Geralis, V.A. Giakoumopoulou, A. Kyriakis, D. Loukas, A. Markou, C. Markou, A. Psallidas, I. Topsis-Giotis

University of Athens, Athens, Greece

A. Panagiotou, N. Saoulidou, E. Stiliaris

University of Ioánnina, Ioánnina, Greece

X. Aslanoglou, I. Evangelou, G. Flouris, C. Foudas, P. Kokkas, N. Manthos, I. Papadopoulos, E. Paradas

Wigner Research Centre for Physics, Budapest, Hungary

G. Bencze, C. Hajdu, P. Hidas, D. Horvath¹⁸, F. Sikler, V. Veszpremi, G. Vesztregombi¹⁹, A.J. Zsigmond

Institute of Nuclear Research ATOMKI, Debrecen, Hungary

N. Beni, S. Czellar, J. Karancsi²⁰, J. Molnar, J. Palinkas, Z. Szillasi

University of Debrecen, Debrecen, Hungary

P. Raics, Z.L. Trocsanyi, B. Ujvari

National Institute of Science Education and Research, Bhubaneswar, India

S.K. Swain

Panjab University, Chandigarh, India

S.B. Beri, V. Bhatnagar, N. Dhingra, R. Gupta, A.K. Kalsi, M. Kaur, M. Mittal, N. Nishu, J.B. Singh

University of Delhi, Delhi, India

Ashok Kumar, Arun Kumar, S. Ahuja, A. Bhardwaj, B.C. Choudhary, A. Kumar, S. Malhotra, M. Naimuddin, K. Ranjan, V. Sharma

Saha Institute of Nuclear Physics, Kolkata, India

S. Banerjee, S. Bhattacharya, K. Chatterjee, S. Dutta, B. Gomber, Sa. Jain, Sh. Jain, R. Khurana, A. Modak, S. Mukherjee, D. Roy, S. Sarkar, M. Sharan

Bhabha Atomic Research Centre, Mumbai, India

A. Abdulsalam, D. Dutta, S. Kailas, V. Kumar, A.K. Mohanty², L.M. Pant, P. Shukla, A. Topkar

Tata Institute of Fundamental Research - EHEP, Mumbai, India

T. Aziz, R.M. Chatterjee, S. Ganguly, S. Ghosh, M. Guchait²¹, A. Gurtu²², G. Kole,

S. Kumar, M. Maity²³, G. Majumder, K. Mazumdar, G.B. Mohanty, B. Parida, K. Sudhakar, N. Wickramage²⁴

Tata Institute of Fundamental Research - HECR, Mumbai, India

S. Banerjee, R.K. Dewanjee, S. Dugad

Institute for Research in Fundamental Sciences (IPM), Tehran, Iran

H. Bakhshiansohi, H. Behnamian, S.M. Etesami²⁵, A. Fahim²⁶, R. Goldouzian, A. Jafari, M. Khakzad, M. Mohammadi Najafabadi, M. Naseri, S. Paktinat Mehdiabadi, B. Safarzadeh²⁷, M. Zeinali

University College Dublin, Dublin, Ireland

M. Felcini, M. Grunewald

INFN Sezione di Bari ^a, Università di Bari ^b, Politecnico di Bari ^c, Bari, Italy

M. Abbrescia^{a,b}, L. Barbone^{a,b}, C. Calabria^{a,b}, S.S. Chhibra^{a,b}, A. Colaleo^a, D. Creanza^{a,c}, N. De Filippis^{a,c}, M. De Palma^{a,b}, L. Fiore^a, G. Iaselli^{a,c}, G. Maggi^{a,c}, M. Maggi^a, S. My^{a,c}, S. Nuzzo^{a,b}, A. Pompili^{a,b}, G. Pugliese^{a,c}, R. Radogna^{a,b,2}, G. Selvaggi^{a,b}, L. Silvestris^{a,2}, G. Singh^{a,b}, R. Venditti^{a,b}, P. Verwilligen^a, G. Zito^a

INFN Sezione di Bologna ^a, Università di Bologna ^b, Bologna, Italy

G. Abbiendi^a, A.C. Benvenuti^a, D. Bonacorsi^{a,b}, S. Braibant-Giacomelli^{a,b}, L. Brigliadori^{a,b}, R. Campanini^{a,b}, P. Capiluppi^{a,b}, A. Castro^{a,b}, F.R. Cavallo^a, G. Codispoti^{a,b}, M. Cuffiani^{a,b}, G.M. Dallavalle^a, F. Fabbri^a, A. Fanfani^{a,b}, D. Fasanella^{a,b}, P. Giacomelli^a, C. Grandi^a, L. Guiducci^{a,b}, S. Marcellini^a, G. Masetti^{a,2}, A. Montanari^a, F.L. Navarria^{a,b}, A. Perrotta^a, F. Primavera^{a,b}, A.M. Rossi^{a,b}, T. Rovelli^{a,b}, G.P. Siroli^{a,b}, N. Tosi^{a,b}, R. Travaglini^{a,b}

INFN Sezione di Catania ^a, Università di Catania ^b, CSFNSM ^c, Catania, Italy

S. Albergo^{a,b}, G. Cappello^a, M. Chiorboli^{a,b}, S. Costa^{a,b}, F. Giordano^{a,c,2}, R. Potenza^{a,b}, A. Tricomi^{a,b}, C. Tuve^{a,b}

INFN Sezione di Firenze ^a, Università di Firenze ^b, Firenze, Italy

G. Barbagli^a, V. Ciulli^{a,b}, C. Civinini^a, R. D'Alessandro^{a,b}, E. Focardi^{a,b}, E. Gallo^a, S. Gonzi^{a,b}, V. Gori^{a,b,2}, P. Lenzi^{a,b}, M. Meschini^a, S. Paoletti^a, G. Sguazzoni^a, A. Tropiano^{a,b}

INFN Laboratori Nazionali di Frascati, Frascati, Italy

L. Benussi, S. Bianco, F. Fabbri, D. Piccolo

INFN Sezione di Genova ^a, Università di Genova ^b, Genova, Italy

F. Ferro^a, M. Lo Vetere^{a,b}, E. Robutti^a, S. Tosi^{a,b}

INFN Sezione di Milano-Bicocca ^a, Università di Milano-Bicocca ^b, Milano, Italy

M.E. Dinardo^{a,b}, S. Fiorendi^{a,b,2}, S. Gennai^{a,2}, R. Gerosa², A. Ghezzi^{a,b}, P. Govoni^{a,b}, M.T. Lucchini^{a,b,2}, S. Malvezzi^a, R.A. Manzoni^{a,b}, A. Martelli^{a,b}, B. Marzocchi, D. Menasce^a, L. Moroni^a, M. Paganoni^{a,b}, D. Pedrini^a, S. Ragazzi^{a,b}, N. Redaelli^a, T. Tabarelli de Fatis^{a,b}

INFN Sezione di Napoli ^a, Università di Napoli 'Federico II' ^b, Università della Basilicata (Potenza) ^c, Università G. Marconi (Roma) ^d, Napoli, Italy

S. Buontempo^a, N. Cavallo^{a,c}, S. Di Guida^{a,d,2}, F. Fabozzi^{a,c}, A.O.M. Iorio^{a,b}, L. Lista^a, S. Meola^{a,d,2}, M. Merola^a, P. Paolucci^{a,2}

INFN Sezione di Padova ^a, Università di Padova ^b, Università di Trento (Trento) ^c, Padova, Italy

P. Azzi^a, N. Bacchetta^a, A. Branca^{a,b}, R. Carlin^{a,b}, P. Checchia^a, M. Dall'Osso^{a,b}, T. Dorigo^a, M. Galanti^{a,b}, F. Gasparini^{a,b}, U. Gasparini^{a,b}, P. Giubilato^{a,b}, F. Gonella^a, A. Gozzelino^a,

K. Kanishchev^{a,c}, S. Lacaprara^a, M. Margoni^{a,b}, A.T. Meneguzzo^{a,b}, F. Montecassiano^a, J. Pazzini^{a,b}, N. Pozzobon^{a,b}, P. Ronchese^{a,b}, F. Simonetto^{a,b}, E. Torassa^a, M. Tosi^{a,b}, S. Vanini^{a,b}, P. Zotto^{a,b}, A. Zucchetta^{a,b}

INFN Sezione di Pavia ^a, Università di Pavia ^b, Pavia, Italy
M. Gabusi^{a,b}, S.P. Ratti^{a,b}, C. Riccardi^{a,b}, P. Salvini^a, P. Vitulo^{a,b}

INFN Sezione di Perugia ^a, Università di Perugia ^b, Perugia, Italy
M. Biasini^{a,b}, G.M. Bilei^a, D. Ciangottini^{a,b}, L. Fanò^{a,b}, P. Lariccia^{a,b}, G. Mantovani^{a,b}, M. Menichelli^a, F. Romeo^{a,b}, A. Saha^a, A. Santocchia^{a,b}, A. Spiezia^{a,b,2}

INFN Sezione di Pisa ^a, Università di Pisa ^b, Scuola Normale Superiore di Pisa ^c, Pisa, Italy
K. Androsov^{a,28}, P. Azzurri^a, G. Bagliesi^a, J. Bernardini^a, T. Boccali^a, G. Broccolo^{a,c}, R. Castaldi^a, M.A. Ciocci^{a,28}, R. Dell'Orso^a, S. Donato^{a,c}, F. Fiori^{a,c}, L. Foà^{a,c}, A. Giassi^a, M.T. Grippo^{a,28}, F. Ligabue^{a,c}, T. Lomtadze^a, L. Martini^{a,b}, A. Messineo^{a,b}, C.S. Moon^{a,29}, F. Palla^{a,2}, A. Rizzi^{a,b}, A. Savoy-Navarro^{a,30}, A.T. Serban^a, P. Spagnolo^a, P. Squillacioti^{a,28}, R. Tenchini^a, G. Tonelli^{a,b}, A. Venturi^a, P.G. Verdini^a, C. Vernieri^{a,c,2}

INFN Sezione di Roma ^a, Università di Roma ^b, Roma, Italy
L. Barone^{a,b}, F. Cavallari^a, D. Del Re^{a,b}, M. Diemoz^a, M. Grassi^{a,b}, C. Jorda^a, E. Longo^{a,b}, F. Margaroli^{a,b}, P. Meridiani^a, F. Micheli^{a,b,2}, S. Nourbakhsh^{a,b}, G. Organtini^{a,b}, R. Paramatti^a, S. Rahatlou^{a,b}, C. Rovelli^a, F. Santanastasio^{a,b}, L. Soffi^{a,b,2}, P. Traczyk^{a,b}

INFN Sezione di Torino ^a, Università di Torino ^b, Università del Piemonte Orientale (Novara) ^c, Torino, Italy
N. Amapane^{a,b}, R. Arcidiacono^{a,c}, S. Argiro^{a,b,2}, M. Arneodo^{a,c}, R. Bellan^{a,b}, C. Biino^a, N. Cartiglia^a, S. Casasso^{a,b,2}, M. Costa^{a,b}, A. Degano^{a,b}, N. Demaria^a, L. Finco^{a,b}, C. Mariotti^a, S. Maselli^a, E. Migliore^{a,b}, V. Monaco^{a,b}, M. Musich^a, M.M. Obertino^{a,c,2}, G. Ortona^{a,b}, L. Pacher^{a,b}, N. Pastrone^a, M. Pelliccioni^a, G.L. Pinna Angioni^{a,b}, A. Potenza^{a,b}, A. Romero^{a,b}, M. Ruspa^{a,c}, R. Sacchi^{a,b}, A. Solano^{a,b}, A. Staiano^a, U. Tamponi^a

INFN Sezione di Trieste ^a, Università di Trieste ^b, Trieste, Italy
S. Belforte^a, V. Candelise^{a,b}, M. Casarsa^a, F. Cossutti^a, G. Della Ricca^{a,b}, B. Gobbo^a, C. La Licata^{a,b}, M. Marone^{a,b}, D. Montanino^{a,b}, A. Schizzi^{a,b,2}, T. Umer^{a,b}, A. Zanetti^a

Kangwon National University, Chunchon, Korea
S. Chang, A. Kropivnitskaya, S.K. Nam

Kyungpook National University, Daegu, Korea
D.H. Kim, G.N. Kim, M.S. Kim, D.J. Kong, S. Lee, Y.D. Oh, H. Park, A. Sakharov, D.C. Son

Chonnam National University, Institute for Universe and Elementary Particles, Kwangju, Korea
J.Y. Kim, S. Song

Korea University, Seoul, Korea
S. Choi, D. Gyun, B. Hong, M. Jo, H. Kim, Y. Kim, B. Lee, K.S. Lee, S.K. Park, Y. Roh

University of Seoul, Seoul, Korea
M. Choi, J.H. Kim, I.C. Park, S. Park, G. Ryu, M.S. Ryu

Sungkyunkwan University, Suwon, Korea
Y. Choi, Y.K. Choi, J. Goh, E. Kwon, J. Lee, H. Seo, I. Yu

Vilnius University, Vilnius, Lithuania
A. Juodagalvis

National Centre for Particle Physics, Universiti Malaya, Kuala Lumpur, Malaysia
J.R. Komaragiri

Centro de Investigacion y de Estudios Avanzados del IPN, Mexico City, Mexico
H. Castilla-Valdez, E. De La Cruz-Burelo, I. Heredia-de La Cruz³¹, R. Lopez-Fernandez,
A. Sanchez-Hernandez

Universidad Iberoamericana, Mexico City, Mexico
S. Carrillo Moreno, F. Vazquez Valencia

Benemerita Universidad Autonoma de Puebla, Puebla, Mexico
I. Pedraza, H.A. Salazar Ibarguen

Universidad Autónoma de San Luis Potosí, San Luis Potosí, Mexico
E. Casimiro Linares, A. Morelos Pineda

University of Auckland, Auckland, New Zealand
D. Kofcheck

University of Canterbury, Christchurch, New Zealand
P.H. Butler, S. Reucroft

National Centre for Physics, Quaid-I-Azam University, Islamabad, Pakistan
A. Ahmad, M. Ahmad, Q. Hassan, H.R. Hoorani, S. Khalid, W.A. Khan, T. Khurshid,
M.A. Shah, M. Shoaib

National Centre for Nuclear Research, Swierk, Poland
H. Bialkowska, M. Bluj³², B. Boimska, T. Frueboes, M. Górski, M. Kazana, K. Nawrocki,
K. Romanowska-Rybinska, M. Szleper, P. Zalewski

Institute of Experimental Physics, Faculty of Physics, University of Warsaw, Warsaw, Poland
G. Brona, K. Bunkowski, M. Cwiok, W. Dominik, K. Doroba, A. Kalinowski, M. Konecki,
J. Krolikowski, M. Misiura, M. Olszewski, W. Wolszczak

Laboratório de Instrumentação e Física Experimental de Partículas, Lisboa, Portugal
P. Bargassa, C. Beirão Da Cruz E Silva, P. Faccioli, P.G. Ferreira Parracho, M. Gallinaro,
F. Nguyen, J. Rodrigues Antunes, J. Seixas, J. Varela, P. Vischia

Joint Institute for Nuclear Research, Dubna, Russia
S. Afanasiev, P. Bunin, I. Golutvin, I. Gorbunov, V. Karjavin, V. Konoplyanikov, G. Kozlov,
A. Lanev, A. Malakhov, V. Matveev³³, P. Moisenz, V. Palichik, V. Perelygin, S. Shmatov,
N. Skatchkov, V. Smirnov, B.S. Yuldashev³⁴, A. Zarubin

Petersburg Nuclear Physics Institute, Gatchina (St. Petersburg), Russia
V. Golovtsov, Y. Ivanov, V. Kim³⁵, P. Levchenko, V. Murzin, V. Oreshkin, I. Smirnov, V. Sulimov,
L. Uvarov, S. Vavilov, A. Vorobyev, An. Vorobyev

Institute for Nuclear Research, Moscow, Russia
Yu. Andreev, A. Dermenev, S. Glinenko, N. Golubev, M. Kirsanov, N. Krasnikov, A. Pashenkov,
D. Tlisov, A. Toropin

Institute for Theoretical and Experimental Physics, Moscow, Russia
V. Epshteyn, V. Gavrilov, N. Lychkovskaya, V. Popov, G. Safronov, S. Semenov, A. Spiridonov,
V. Stolin, E. Vlasov, A. Zhokin

P.N. Lebedev Physical Institute, Moscow, Russia

V. Andreev, M. Azarkin, I. Dremin, M. Kirakosyan, A. Leonidov, G. Mesyats, S.V. Rusakov, A. Vinogradov

Skobeltsyn Institute of Nuclear Physics, Lomonosov Moscow State University, Moscow, Russia

A. Belyaev, E. Boos, V. Bunichev, M. Dubinin⁷, L. Dudko, A. Ershov, V. Klyukhin, O. Kodolova, I. Lokhtin, S. Obraztsov, S. Petrushanko, V. Savrin, A. Snigirev

State Research Center of Russian Federation, Institute for High Energy Physics, Protvino, Russia

I. Azhgirey, I. Bayshev, S. Bitioukov, V. Kachanov, A. Kalinin, D. Konstantinov, V. Krychkine, V. Petrov, R. Ryutin, A. Sobol, L. Tourtchanovitch, S. Troshin, N. Tyurin, A. Uzunian, A. Volkov

University of Belgrade, Faculty of Physics and Vinca Institute of Nuclear Sciences, Belgrade, Serbia

P. Adzic³⁶, M. Dordevic, M. Ekmedzic, J. Milosevic

Centro de Investigaciones Energéticas Medioambientales y Tecnológicas (CIEMAT), Madrid, Spain

J. Alcaraz Maestre, C. Battilana, E. Calvo, M. Cerrada, M. Chamizo Llatas², N. Colino, B. De La Cruz, A. Delgado Peris, D. Domínguez Vázquez, A. Escalante Del Valle, C. Fernandez Bedoya, J.P. Fernández Ramos, J. Flix, M.C. Fouz, P. Garcia-Abia, O. Gonzalez Lopez, S. Goy Lopez, J.M. Hernandez, M.I. Josa, G. Merino, E. Navarro De Martino, A. Pérez-Calero Yzquierdo, J. Puerta Pelayo, A. Quintario Olmeda, I. Redondo, L. Romero, M.S. Soares

Universidad Autónoma de Madrid, Madrid, Spain

C. Albajar, J.F. de Trocóniz, M. Missiroli

Universidad de Oviedo, Oviedo, Spain

H. Brun, J. Cuevas, J. Fernandez Menendez, S. Folgueras, I. Gonzalez Caballero, L. Lloret Iglesias

Instituto de Física de Cantabria (IFCA), CSIC-Universidad de Cantabria, Santander, Spain

J.A. Brochero Cifuentes, I.J. Cabrillo, A. Calderon, J. Duarte Campderros, M. Fernandez, G. Gomez, A. Graziano, A. Lopez Virto, J. Marco, R. Marco, C. Martinez Rivero, F. Matorras, F.J. Munoz Sanchez, J. Piedra Gomez, T. Rodrigo, A.Y. Rodríguez-Marrero, A. Ruiz-Jimeno, L. Scodellaro, I. Vila, R. Vilar Cortabitarte

CERN, European Organization for Nuclear Research, Geneva, Switzerland

D. Abbaneo, E. Auffray, G. Auzinger, M. Bachtis, P. Baillon, A.H. Ball, D. Barney, A. Benaglia, J. Bendavid, L. Benhabib, J.F. Benitez, C. Bernet⁸, G. Bianchi, P. Bloch, A. Bocci, A. Bonato, O. Bondi, C. Botta, H. Breuker, T. Camporesi, G. Cerminara, T. Christiansen, S. Colafranceschi³⁷, M. D'Alfonso, D. d'Enterria, A. Dabrowski, A. David, F. De Guio, A. De Roeck, S. De Visscher, M. Dobson, N. Dupont-Sagorin, A. Elliott-Peisert, J. Eugster, G. Franzoni, W. Funk, M. Giffels, D. Gigi, K. Gill, D. Giordano, M. Girone, F. Glege, R. Guida, S. Gundacker, M. Guthoff, J. Hammer, M. Hansen, P. Harris, J. Hegeman, V. Innocente, P. Janot, K. Kousouris, K. Krajczar, P. Lecoq, C. Lourenço, N. Magini, L. Malgeri, M. Mannelli, L. Masetti, F. Meijers, S. Mersi, E. Meschi, F. Moortgat, S. Morovic, M. Mulders, P. Musella, L. Orsini, L. Pape, E. Perez, L. Perrozzi, A. Petrilli, G. Petrucciani, A. Pfeiffer, M. Pierini, M. Pimiä, D. Piparo, M. Plagge, A. Racz, G. Rolandi³⁸, M. Rovere, H. Sakulin, C. Schäfer, C. Schwick, S. Sekmen, A. Sharma, P. Siegrist, P. Silva, M. Simon, P. Sphicas³⁹, D. Spiga, J. Steggemann, B. Stieger, M. Stoye, D. Treille, A. Tsirou, G.I. Veres¹⁹, J.R. Vlimant, N. Wardle, H.K. Wöhri, W.D. Zeuner

Paul Scherrer Institut, Villigen, Switzerland

W. Bertl, K. Deiters, W. Erdmann, R. Horisberger, Q. Ingram, H.C. Kaestli, S. König, D. Kotlinski, U. Langenegger, D. Renker, T. Rohe

Institute for Particle Physics, ETH Zurich, Zurich, Switzerland

F. Bachmair, L. Bäni, L. Bianchini, P. Bortignon, M.A. Buchmann, B. Casal, N. Chanon, A. Deisher, G. Dissertori, M. Dittmar, M. Donegà, M. Dünser, P. Eller, C. Grab, D. Hits, W. Lustermann, B. Mangano, A.C. Marini, P. Martinez Ruiz del Arbol, D. Meister, N. Mohr, C. Nägeli⁴⁰, P. Nef, F. Nessi-Tedaldi, F. Pandolfi, F. Pauss, M. Peruzzi, M. Quittnat, L. Rebane, F.J. Ronga, M. Rossini, A. Starodumov⁴¹, M. Takahashi, K. Theofilatos, R. Wallny, H.A. Weber

Universität Zürich, Zurich, Switzerland

C. Amsler⁴², M.F. Canelli, V. Chiochia, A. De Cosa, A. Hinzmann, T. Hreus, M. Ivova Rikova, B. Kilminster, B. Millan Mejias, J. Ngadiuba, P. Robmann, H. Snoek, S. Taroni, M. Verzetti, Y. Yang

National Central University, Chung-Li, Taiwan

M. Cardaci, K.H. Chen, C. Ferro, C.M. Kuo, W. Lin, Y.J. Lu, R. Volpe, S.S. Yu

National Taiwan University (NTU), Taipei, Taiwan

P. Chang, Y.H. Chang, Y.W. Chang, Y. Chao, K.F. Chen, P.H. Chen, C. Dietz, U. Grundler, W.-S. Hou, K.Y. Kao, Y.J. Lei, Y.F. Liu, R.-S. Lu, D. Majumder, E. Petrakou, Y.M. Tzeng, R. Wilken

Chulalongkorn University, Bangkok, Thailand

B. Asavapibhop, N. Srimanobhas, N. Suwonjandee

Cukurova University, Adana, Turkey

A. Adiguzel, M.N. Bakirci⁴³, S. Cerci⁴⁴, C. Dozen, I. Dumanoglu, E. Eskut, S. Girgis, G. Gokbulut, E. Gurpinar, I. Hos, E.E. Kangal, A. Kayis Topaksu, G. Onengut⁴⁵, K. Ozdemir, S. Ozturk⁴³, A. Polatoz, K. Sogut⁴⁶, D. Sunar Cerci⁴⁴, B. Tali⁴⁴, H. Topakli⁴³, M. Vergili

Middle East Technical University, Physics Department, Ankara, Turkey

I.V. Akin, B. Bilin, S. Bilmis, H. Gamsizkan, G. Karapinar⁴⁷, K. Ocalan, U.E. Surat, M. Yalvac, M. Zeyrek

Bogazici University, Istanbul, Turkey

E. Gümez, B. Isildak⁴⁸, M. Kaya⁴⁹, O. Kaya⁴⁹

Istanbul Technical University, Istanbul, Turkey

H. Bahtiyar⁵⁰, E. Barlas, K. Cankocak, F.I. Vardarli, M. Yücel

National Scientific Center, Kharkov Institute of Physics and Technology, Kharkov, Ukraine

L. Levchuk, P. Sorokin

University of Bristol, Bristol, United Kingdom

J.J. Brooke, E. Clement, D. Cussans, H. Flacher, R. Frazier, J. Goldstein, M. Grimes, G.P. Heath, H.F. Heath, J. Jacob, L. Kreczko, C. Lucas, Z. Meng, D.M. Newbold⁵¹, S. Paramesvaran, A. Poll, S. Senkin, V.J. Smith, T. Williams

Rutherford Appleton Laboratory, Didcot, United Kingdom

K.W. Bell, A. Belyaev⁵², C. Brew, R.M. Brown, D.J.A. Cockerill, J.A. Coughlan, K. Harder, S. Harper, E. Olaiya, D. Petyt, C.H. Shepherd-Themistocleous, A. Thea, I.R. Tomalin, W.J. Womersley, S.D. Worm

Imperial College, London, United Kingdom

M. Baber, R. Bainbridge, O. Buchmuller, D. Burton, D. Colling, N. Cripps, M. Cutajar,

P. Dauncey, G. Davies, M. Della Negra, P. Dunne, W. Ferguson, J. Fulcher, D. Futyan, A. Gilbert, G. Hall, G. Iles, M. Jarvis, G. Karapostoli, M. Kenzie, R. Lane, R. Lucas⁵¹, L. Lyons, A.-M. Magnan, S. Malik, J. Marrouche, B. Mathias, J. Nash, A. Nikitenko⁴¹, J. Pela, M. Pesaresi, K. Petridis, D.M. Raymond, S. Rogerson, A. Rose, C. Seez, P. Sharp[†], A. Tapper, M. Vazquez Acosta, T. Virdee

Brunel University, Uxbridge, United Kingdom

J.E. Cole, P.R. Hobson, A. Khan, P. Kyberd, D. Leggat, D. Leslie, W. Martin, I.D. Reid, P. Symonds, L. Teodorescu, M. Turner

Baylor University, Waco, USA

J. Dittmann, K. Hatakeyama, A. Kasmi, H. Liu, T. Scarborough

The University of Alabama, Tuscaloosa, USA

O. Charaf, S.I. Cooper, C. Henderson, P. Rumerio

Boston University, Boston, USA

A. Avetisyan, T. Bose, C. Fantasia, A. Heister, P. Lawson, C. Richardson, J. Rohlf, D. Sperka, J. St. John, L. Sulak

Brown University, Providence, USA

J. Alimena, S. Bhattacharya, G. Christopher, D. Cutts, Z. Demiragli, A. Ferapontov, A. Garabedian, U. Heintz, S. Jabeen, G. Kukartsev, E. Laird, G. Landsberg, M. Luk, M. Narain, M. Segala, T. Sinthuprasith, T. Speer, J. Swanson

University of California, Davis, Davis, USA

R. Breedon, G. Breto, M. Calderon De La Barca Sanchez, S. Chauhan, M. Chertok, J. Conway, R. Conway, P.T. Cox, R. Erbacher, M. Gardner, W. Ko, R. Lander, T. Miceli, M. Mulhearn, D. Pellett, J. Pilot, F. Ricci-Tam, M. Searle, S. Shalhout, J. Smith, M. Squires, D. Stolp, M. Tripathi, S. Wilbur, R. Yohay

University of California, Los Angeles, USA

R. Cousins, P. Everaerts, C. Farrell, J. Hauser, M. Ignatenko, G. Rakness, E. Takasugi, V. Valuev, M. Weber

University of California, Riverside, Riverside, USA

J. Babb, R. Clare, J. Ellison, J.W. Gary, G. Hanson, J. Heilman, P. Jandir, E. Kennedy, F. Lacroix, H. Liu, O.R. Long, A. Luthra, M. Malberti, H. Nguyen, A. Shrinivas, S. Sumowidagdo, S. Wimpenny

University of California, San Diego, La Jolla, USA

J.G. Branson, G.B. Cerati, S. Cittolin, R.T. D'Agnolo, D. Evans, A. Holzner, R. Kelley, D. Kovalevskyi, M. Lebourgeois, J. Letts, I. Macneill, D. Olivito, S. Padhi, C. Palmer, M. Pieri, M. Sani, V. Sharma, S. Simon, E. Sudano, M. Tadel, Y. Tu, A. Vartak, F. Würthwein, A. Yagil, J. Yoo

University of California, Santa Barbara, Santa Barbara, USA

D. Barge, J. Bradmiller-Feld, C. Campagnari, T. Danielson, A. Dishaw, K. Flowers, M. Franco Sevilla, P. Geffert, C. George, F. Golf, L. Gouskos, J. Incandela, C. Justus, N. Mccoll, J. Richman, D. Stuart, W. To, C. West

California Institute of Technology, Pasadena, USA

A. Apresyan, A. Bornheim, J. Bunn, Y. Chen, E. Di Marco, J. Duarte, A. Mott, H.B. Newman, C. Pena, C. Rogan, M. Spiropulu, V. Timciuc, R. Wilkinson, S. Xie, R.Y. Zhu

Carnegie Mellon University, Pittsburgh, USA

V. Azzolini, A. Calamba, T. Ferguson, Y. Iiyama, M. Paulini, J. Russ, H. Vogel, I. Vorobiev

University of Colorado at Boulder, Boulder, USA

J.P. Cumalat, B.R. Drell, W.T. Ford, A. Gaz, E. Luiggi Lopez, U. Nauenberg, J.G. Smith, K. Stenson, K.A. Ulmer, S.R. Wagner

Cornell University, Ithaca, USA

J. Alexander, A. Chatterjee, J. Chu, S. Dittmer, N. Eggert, W. Hopkins, B. Kreis, N. Mirman, G. Nicolas Kaufman, J.R. Patterson, A. Ryd, E. Salvati, L. Skinnari, W. Sun, W.D. Teo, J. Thom, J. Thompson, J. Tucker, Y. Weng, L. Winstrom, P. Wittich

Fairfield University, Fairfield, USA

D. Winn

Fermi National Accelerator Laboratory, Batavia, USA

S. Abdullin, M. Albrow, J. Anderson, G. Apollinari, L.A.T. Bauerick, A. Beretvas, J. Berryhill, P.C. Bhat, K. Burkett, J.N. Butler, H.W.K. Cheung, F. Chlebana, S. Cihangir, V.D. Elvira, I. Fisk, J. Freeman, E. Gottschalk, L. Gray, D. Green, S. Grünendahl, O. Gutsche, J. Hanlon, D. Hare, R.M. Harris, J. Hirschauer, B. Hooberman, S. Jindariani, M. Johnson, U. Joshi, K. Kaadze, B. Klima, S. Kwan, J. Linacre, D. Lincoln, R. Lipton, T. Liu, J. Lykken, K. Maeshima, J.M. Marraffino, V.I. Martinez Outschoorn, S. Maruyama, D. Mason, P. McBride, K. Mishra, S. Mrenna, Y. Musienko³³, S. Nahn, C. Newman-Holmes, V. O'Dell, O. Prokofyev, E. Sexton-Kennedy, S. Sharma, A. Soha, W.J. Spalding, L. Spiegel, L. Taylor, S. Tkaczyk, N.V. Tran, L. Uplegger, E.W. Vaandering, R. Vidal, A. Whitbeck, J. Whitmore, F. Yang

University of Florida, Gainesville, USA

D. Acosta, P. Avery, D. Bourilkov, M. Carver, T. Cheng, D. Curry, S. Das, M. De Gruttola, G.P. Di Giovanni, R.D. Field, M. Fisher, I.K. Furic, J. Hugon, J. Konigsberg, A. Korytov, T. Kypreos, J.F. Low, K. Matchev, P. Milenovic⁵³, G. Mitselmakher, L. Muniz, A. Rinkevicius, L. Shchutska, N. Skhirtladze, M. Snowball, J. Yelton, M. Zakaria

Florida International University, Miami, USA

V. Gaultney, S. Hewamanage, S. Linn, P. Markowitz, G. Martinez, J.L. Rodriguez

Florida State University, Tallahassee, USA

T. Adams, A. Askew, J. Bochenek, B. Diamond, J. Haas, S. Hagopian, V. Hagopian, K.F. Johnson, H. Prosper, V. Veeraraghavan, M. Weinberg

Florida Institute of Technology, Melbourne, USA

M.M. Baarmand, M. Hohlmann, H. Kalakhety, F. Yumiceva

University of Illinois at Chicago (UIC), Chicago, USA

M.R. Adams, L. Apanasevich, V.E. Bazterra, D. Berry, R.R. Betts, I. Bucinskaite, R. Cavanaugh, O. Evdokimov, L. Gauthier, C.E. Gerber, D.J. Hofman, S. Khalatyan, P. Kurt, D.H. Moon, C. O'Brien, C. Silkworth, P. Turner, N. Varelas

The University of Iowa, Iowa City, USA

E.A. Albayrak⁵⁰, B. Bilki⁵⁴, W. Clarida, K. Dilsiz, F. Duru, M. Haytmyradov, J.-P. Merlo, H. Mermerkaya⁵⁵, A. Mestvirishvili, A. Moeller, J. Nachtman, H. Ogul, Y. Onel, F. Ozok⁵⁰, A. Penzo, R. Rahmat, S. Sen, P. Tan, E. Tiras, J. Wetzel, T. Yetkin⁵⁶, K. Yi

Johns Hopkins University, Baltimore, USA

B.A. Barnett, B. Blumenfeld, S. Bolognesi, D. Fehling, A.V. Gritsan, P. Maksimovic, C. Martin, M. Swartz

The University of Kansas, Lawrence, USA

P. Baringer, A. Bean, G. Benelli, C. Bruner, J. Gray, R.P. Kenny III, M. Murray, D. Noonan, S. Sanders, J. Sekaric, R. Stringer, Q. Wang, J.S. Wood

Kansas State University, Manhattan, USA

A.F. Barfuss, I. Chakaberia, A. Ivanov, S. Khalil, M. Makouski, Y. Maravin, L.K. Saini, S. Shrestha, I. Svintradze

Lawrence Livermore National Laboratory, Livermore, USA

J. Gronberg, D. Lange, F. Rebassoo, D. Wright

University of Maryland, College Park, USA

A. Baden, B. Calvert, S.C. Eno, J.A. Gomez, N.J. Hadley, R.G. Kellogg, T. Kolberg, Y. Lu, M. Marionneau, A.C. Mignerey, K. Pedro, A. Skuja, M.B. Tonjes, S.C. Tonwar

Massachusetts Institute of Technology, Cambridge, USA

A. Apyan, R. Barbieri, G. Bauer, W. Busza, I.A. Cali, M. Chan, L. Di Matteo, V. Dutta, G. Gomez Ceballos, M. Goncharov, D. Gulhan, M. Klute, Y.S. Lai, Y.-J. Lee, A. Levin, P.D. Luckey, T. Ma, C. Paus, D. Ralph, C. Roland, G. Roland, G.S.F. Stephans, F. Stöckli, K. Sumorok, D. Velicanu, J. Veverka, B. Wyslouch, M. Yang, M. Zanetti, V. Zhukova

University of Minnesota, Minneapolis, USA

B. Dahmes, A. De Benedetti, A. Gude, S.C. Kao, K. Klapoetke, Y. Kubota, J. Mans, N. Pastika, R. Rusack, A. Singovsky, N. Tambe, J. Turkewitz

University of Mississippi, Oxford, USA

J.G. Acosta, S. Oliveros

University of Nebraska-Lincoln, Lincoln, USA

E. Avdeeva, K. Bloom, S. Bose, D.R. Claes, A. Dominguez, R. Gonzalez Suarez, J. Keller, D. Knowlton, I. Kravchenko, J. Lazo-Flores, S. Malik, F. Meier, G.R. Snow

State University of New York at Buffalo, Buffalo, USA

J. Dolen, A. Godshalk, I. Iashvili, A. Kharchilava, A. Kumar, S. Rappoccio

Northeastern University, Boston, USA

G. Alverson, E. Barberis, D. Baumgartel, M. Chasco, J. Haley, A. Massironi, D.M. Morse, D. Nash, T. Orimoto, D. Trocino, D. Wood, J. Zhang

Northwestern University, Evanston, USA

K.A. Hahn, A. Kubik, N. Mucia, N. Odell, B. Pollack, A. Pozdnyakov, M. Schmitt, S. Stoynev, K. Sung, M. Velasco, S. Won

University of Notre Dame, Notre Dame, USA

A. Brinkerhoff, K.M. Chan, A. Drozdetskiy, M. Hildreth, C. Jessop, D.J. Karmgard, N. Kellams, K. Lannon, W. Luo, S. Lynch, N. Marinelli, T. Pearson, M. Planer, R. Ruchti, N. Valls, M. Wayne, M. Wolf, A. Woodard

The Ohio State University, Columbus, USA

L. Antonelli, J. Brinson, B. Bylsma, L.S. Durkin, S. Flowers, C. Hill, R. Hughes, K. Kotov, T.Y. Ling, D. Puigh, M. Rodenburg, G. Smith, C. Vuosalo, B.L. Winer, H. Wolfe, H.W. Wulsin

Princeton University, Princeton, USA

E. Berry, O. Driga, P. Elmer, P. Hebda, A. Hunt, S.A. Koay, P. Lujan, D. Marlow, T. Medvedeva, M. Mooney, J. Olsen, P. Piroué, X. Quan, H. Saka, D. Stickland², C. Tully, J.S. Werner, S.C. Zenz, A. Zuranski

University of Puerto Rico, Mayaguez, USA
E. Brownson, H. Mendez, J.E. Ramirez Vargas

Purdue University, West Lafayette, USA
E. Alagoz, V.E. Barnes, D. Benedetti, G. Bolla, D. Bortoletto, M. De Mattia, A. Everett, Z. Hu, M.K. Jha, M. Jones, K. Jung, M. Kress, N. Leonardo, D. Lopes Pegna, V. Maroussov, P. Merkel, D.H. Miller, N. Neumeister, B.C. Radburn-Smith, X. Shi, I. Shipsey, D. Silvers, A. Svyatkovskiy, F. Wang, W. Xie, L. Xu, H.D. Yoo, J. Zablocki, Y. Zheng

Purdue University Calumet, Hammond, USA
N. Parashar, J. Stupak

Rice University, Houston, USA
A. Adair, B. Akgun, K.M. Ecklund, F.J.M. Geurts, W. Li, B. Michlin, B.P. Padley, R. Redjimi, J. Roberts, J. Zabel

University of Rochester, Rochester, USA
B. Betchart, A. Bodek, R. Covarelli, P. de Barbaro, R. Demina, Y. Eshaq, T. Ferbel, A. Garcia-Bellido, P. Goldenzweig, J. Han, A. Harel, A. Khukhunaishvili, D.C. Miner, G. Petrillo, D. Vishnevskiy

The Rockefeller University, New York, USA
R. Ciesielski, L. Demortier, K. Goulianos, G. Lungu, C. Mesropian

Rutgers, The State University of New Jersey, Piscataway, USA
S. Arora, A. Barker, J.P. Chou, C. Contreras-Campana, E. Contreras-Campana, D. Duggan, D. Ferencek, Y. Gershtein, R. Gray, E. Halkiadakis, D. Hidas, A. Lath, S. Panwalkar, M. Park, R. Patel, V. Rekovic, S. Salur, S. Schnetzer, C. Seitz, S. Somalwar, R. Stone, S. Thomas, P. Thomassen, M. Walker

University of Tennessee, Knoxville, USA
K. Rose, S. Spanier, A. York

Texas A&M University, College Station, USA
O. Bouhali⁵⁷, R. Eusebi, W. Flanagan, J. Gilmore, T. Kamon⁵⁸, V. Khotilovich, V. Krutelyov, R. Montalvo, I. Osipenkov, Y. Pakhotin, A. Perloff, J. Roe, A. Rose, A. Safonov, T. Sakuma, I. Suarez, A. Tatarinov

Texas Tech University, Lubbock, USA
N. Akchurin, C. Cowden, J. Damgov, C. Dragoiu, P.R. Dudero, J. Faulkner, K. Kovitanggoon, S. Kunori, S.W. Lee, T. Libeiro, I. Volobouev

Vanderbilt University, Nashville, USA
E. Appelt, A.G. Delannoy, S. Greene, A. Gurrola, W. Johns, C. Maguire, Y. Mao, A. Melo, M. Sharma, P. Sheldon, B. Snook, S. Tuo, J. Velkovska

University of Virginia, Charlottesville, USA
M.W. Arenton, S. Boutle, B. Cox, B. Francis, J. Goodell, R. Hirosky, A. Ledovskoy, H. Li, C. Lin, C. Neu, J. Wood

Wayne State University, Detroit, USA
S. Gollapinni, R. Harr, P.E. Karchin, C. Kottachchi Kankanamge Don, P. Lamichhane, J. Sturdy

University of Wisconsin, Madison, USA
D.A. Belknap, D. Carlsmith, M. Cepeda, S. Dasu, S. Duric, E. Friis, R. Hall-Wilton, M. Herndon,

A. Hervé, P. Klabbers, J. Klukas, A. Lanaro, C. Lazaridis, A. Levine, R. Loveless, A. Mohapatra, I. Ojalvo, T. Perry, G.A. Pierro, G. Polese, I. Ross, T. Sarangi, A. Savin, W.H. Smith, N. Woods

†: Deceased

- 1: Also at Vienna University of Technology, Vienna, Austria
- 2: Also at CERN, European Organization for Nuclear Research, Geneva, Switzerland
- 3: Also at Institut Pluridisciplinaire Hubert Curien, Université de Strasbourg, Université de Haute Alsace Mulhouse, CNRS/IN2P3, Strasbourg, France
- 4: Also at National Institute of Chemical Physics and Biophysics, Tallinn, Estonia
- 5: Also at Skobeltsyn Institute of Nuclear Physics, Lomonosov Moscow State University, Moscow, Russia
- 6: Also at Universidade Estadual de Campinas, Campinas, Brazil
- 7: Also at California Institute of Technology, Pasadena, USA
- 8: Also at Laboratoire Leprince-Ringuet, Ecole Polytechnique, IN2P3-CNRS, Palaiseau, France
- 9: Also at Suez University, Suez, Egypt
- 10: Also at Cairo University, Cairo, Egypt
- 11: Also at Fayoum University, El-Fayoum, Egypt
- 12: Also at British University in Egypt, Cairo, Egypt
- 13: Now at Ain Shams University, Cairo, Egypt
- 14: Also at Université de Haute Alsace, Mulhouse, France
- 15: Also at Joint Institute for Nuclear Research, Dubna, Russia
- 16: Also at Brandenburg University of Technology, Cottbus, Germany
- 17: Also at The University of Kansas, Lawrence, USA
- 18: Also at Institute of Nuclear Research ATOMKI, Debrecen, Hungary
- 19: Also at Eötvös Loránd University, Budapest, Hungary
- 20: Also at University of Debrecen, Debrecen, Hungary
- 21: Also at Tata Institute of Fundamental Research - HECR, Mumbai, India
- 22: Now at King Abdulaziz University, Jeddah, Saudi Arabia
- 23: Also at University of Visva-Bharati, Santiniketan, India
- 24: Also at University of Ruhuna, Matara, Sri Lanka
- 25: Also at Isfahan University of Technology, Isfahan, Iran
- 26: Also at Sharif University of Technology, Tehran, Iran
- 27: Also at Plasma Physics Research Center, Science and Research Branch, Islamic Azad University, Tehran, Iran
- 28: Also at Università degli Studi di Siena, Siena, Italy
- 29: Also at Centre National de la Recherche Scientifique (CNRS) - IN2P3, Paris, France
- 30: Also at Purdue University, West Lafayette, USA
- 31: Also at Universidad Michoacana de San Nicolas de Hidalgo, Morelia, Mexico
- 32: Also at National Centre for Nuclear Research, Swierk, Poland
- 33: Also at Institute for Nuclear Research, Moscow, Russia
- 34: Also at Institute of Nuclear Physics of the Uzbekistan Academy of Sciences, Tashkent, Uzbekistan
- 35: Also at St. Petersburg State Polytechnical University, St. Petersburg, Russia
- 36: Also at Faculty of Physics, University of Belgrade, Belgrade, Serbia
- 37: Also at Facoltà Ingegneria, Università di Roma, Roma, Italy
- 38: Also at Scuola Normale e Sezione dell'INFN, Pisa, Italy
- 39: Also at University of Athens, Athens, Greece
- 40: Also at Paul Scherrer Institut, Villigen, Switzerland
- 41: Also at Institute for Theoretical and Experimental Physics, Moscow, Russia
- 42: Also at Albert Einstein Center for Fundamental Physics, Bern, Switzerland

- 43: Also at Gaziosmanpasa University, Tokat, Turkey
- 44: Also at Adiyaman University, Adiyaman, Turkey
- 45: Also at Cag University, Mersin, Turkey
- 46: Also at Mersin University, Mersin, Turkey
- 47: Also at Izmir Institute of Technology, Izmir, Turkey
- 48: Also at Ozyegin University, Istanbul, Turkey
- 49: Also at Kafkas University, Kars, Turkey
- 50: Also at Mimar Sinan University, Istanbul, Istanbul, Turkey
- 51: Also at Rutherford Appleton Laboratory, Didcot, United Kingdom
- 52: Also at School of Physics and Astronomy, University of Southampton, Southampton, United Kingdom
- 53: Also at University of Belgrade, Faculty of Physics and Vinca Institute of Nuclear Sciences, Belgrade, Serbia
- 54: Also at Argonne National Laboratory, Argonne, USA
- 55: Also at Erzincan University, Erzincan, Turkey
- 56: Also at Yildiz Technical University, Istanbul, Turkey
- 57: Also at Texas A&M University at Qatar, Doha, Qatar
- 58: Also at Kyungpook National University, Daegu, Korea